2022-11-27

Structural and functional magnetic resonance imaging correlates of fatigue and dual-task performance in progressive multiple sclerosis

Preziosa, P

10.1007/s00415-022-11486-0
Journal of Neurology
Springer Science and Business Media LLC

Accepted for publication in Journal of Neurology 2022

doi: 10.1007/s00415-022-11486-0. Online ahead of print.

STRUCTURAL AND FUNCTIONAL MAGNETIC RESONANCE IMAGING CORRELATES OF FATIGUE AND DUAL-TASK PERFORMANCE IN PROGRESSIVE MULTIPLE SCLEROSIS

[1,2,3]Paolo Preziosa, [1,2,3]Maria A. Rocca, [1]Elisabetta Pagani, [1]Paola Valsasina, [4,5]Maria Pia Amato, [6,7]Giampaolo Brichetto, [8]Nicolò Bruschi, [9,10]Jeremy Chataway, [11,12]Nancy D. Chiaravalloti, [13]Gary Cutter, [14]Ulrik Dalgas, [11,12]John DeLuca, [9,10]Rachel Farrell, [15]Peter Feys, [16]Jennifer Freeman, [8,17]Matilde Inglese, [1]Alessandro Meani, [18]Cecilia Meza, [19]Robert W. Motl, [20]Amber Salter, [11,12]Brian M. Sandroff, [18*]Anthony Feinstein, [1,2,3*]Massimo Filippi, CogEx Research Team.

[1]Neuroimaging Research Unit, Division of Neuroscience, [2]Neurology Unit, San Raffaele Scientific Institute, [3]Vita-Salute San Raffaele University, Via Olgettina 60, 20132 Milan, Italy
[4]Department NEUROFARBA, Section Neurosciences, University of Florence, Largo Brambilla 3, 50134, Florence, Italy
[5]IRCCS Fondazione Don Carlo Gnocchi, Florence, Italy
[6]Scientific Research Area, Italian Multiple Sclerosis Foundation (FISM), via Operai 40, 16149, Genoa, Italy
[7]AISM Rehabilitation Service, Italian Multiple Sclerosis Society, Via Operai 30, 16149, Genoa, Italy
[8]Department of Neuroscience, Rehabilitation, Ophthalmology, Genetics, Maternal and Child Health, and Center of Excellence for Biomedical Research, University of Genoa, Genoa, Italy.
[9] Queen Square Multiple Sclerosis Centre, Department of Neuroinflammation, UCL Queen Square Institute of Neurology, Faculty of Brain Sciences, University College London, London, WC1B 5EH, UK
[10]National Institute for Health Research, University College London Hospitals, Biomedical Research Centre, London, W1T 7DN, UK
[11]Kessler Foundation, West Orange, NJ, USA
[12]Department of Physical Medicine & Rehabilitation, Rutgers NJ Medical School, Newark, NJ, USA
[13]Department of Biostatistics, University of Alabama at Birmingham, Birmingham, AL, USA
[14]Exercise Biology, Department of Public Health, Aarhus University, Dalgas Avenue 4, DK-8000 Aarhus, Denmark
[15]REVAL, Faculty of Rehabilitation Sciences, Hasselt University, Diepenbeek, Belgium
[16]Faculty of Health, School of Health Professions, University of Plymouth, Devon, UK
[17]IRCCS Ospedale Policlinico San Martino, Genoa
[18]Department of Psychiatry, University of Toronto and Sunnybrook Health Sciences Centre, Toronto, ON M5R 3B6, Canada
[19]Department of Kinesiology and Nutrition, University of Illinois Chicago, Chicago, IL, USA
[20]Department of Neurology, Section on Statistical Planning and Analysis, UT Southwestern Medical Center, Dallas, TX, USA

*Contributed equally to this work.

Running title: Fatigue and dual-task substrates in PMS.

Manuscript type: Original Communication.
Abstract word count: 250; **Manuscript word count:** 5387.
Number of Tables: 5; **Number of Figures:** 3; **Number of references:** 54.
Supplemental Material: Supplementary Methods.

Keywords: multiple sclerosis, fatigue, dual-task, atrophy, tractography, resting state, MRI.

Correspondence to: Massimo Filippi, MD, FEAN, FAAN
Full Professor of Neurology, Vita-Salute San Raffaele University, Chair, Neurology Unit, Chair, Neurorehabilitation Unit, Director, Neurophysiology Service, Director, MS Center, Director, Neuroimaging Research Unit, Division of Neuroscience, IRCCS San Raffaele Scientific Institute, Via Olgettina, 60, 20132 Milan, Italy; email: filippi.massimo@hsr.it

Abstract

Background. Frontal cortico-subcortical dysfunction may contribute to fatigue and dual-task impairment of walking and cognition in progressive multiple sclerosis (PMS).

Purpose. To explore the associations among fatigue, dual-task performance and structural and functional abnormalities of frontal cortico-subcortical network in PMS.

Methods. Brain 3T structural and functional MRI sequences, Modified Fatigue Impact Scale (MFIS), dual-task motor and cognitive performances were obtained from 57 PMS patients and 10 healthy controls (HC). The associations of thalamic, caudate nucleus and dorsolateral prefrontal cortex (DLPFC) atrophy, microstructural abnormalities of their connections and their resting state effective connectivity (RS-EC) with fatigue and dual-task performance were investigated using random forest.

Results. Thirty-seven PMS patients were fatigued (F) (MFIS≥38). Compared to HC, non-fatigued (nF) and F-PMS patients had significantly worse dual-task performance ($p \leq 0.002$). Predictors of fatigue (out-of-bag [OOB]-accuracy=0.754) and its severity (OOB-R^2=0.247) were higher Expanded Disability Status scale (EDSS) score, lower RS-EC from left-caudate nucleus to left-DLPFC, lower fractional anisotropy between left-caudate nucleus and left-thalamus, higher mean diffusivity between right-caudate nucleus and right-thalamus, and longer disease duration. Microstructural abnormalities in connections among thalami, caudate nuclei and DLPFC, mainly left-lateralized in nF-PMS and more bilateral in F-PMS, higher RS-EC from left-DLPFC to right-DLPFC in nF-PMS and lower RS-EC from left-caudate nucleus to left-DLPFC in F-PMS, higher EDSS score, higher WM lesion volume, and lower cortical volume predicted worse dual-task performances (OOB-R^2 from 0.426 to 0.530).

Conclusions. In PMS, structural and functional frontal cortico-subcortical abnormalities contribute to fatigue and worse dual-task performance, with different patterns according to the presence of fatigue.

Introduction

Fatigue is a frequent and disabling symptom of multiple sclerosis (MS), affecting up to 80% of patients, especially those with progressive (P) forms of the disease (PMS), with highly detrimental impact of their daily-life activities and quality of life [1]. Functional magnetic resonance imaging (MRI) studies in MS patients reporting fatigue have consistently revealed an abnormal recruitment of several brain regions, mainly involving fronto-parietal cortices and the basal ganglia, which are part of the sensorimotor network [2-4]. Growing evidence has also highlighted the role of focal white matter (WM) lesions, microstructural WM abnormalities and gray matter (GM) atrophy of networks including prefrontal cortices, thalamus and caudate nucleus in the pathogenesis of MS-related fatigue [2-4].

Dual-task is the ability to perform two activities (e.g., motor and cognitive) simultaneously [5-9]. Due to 'cognitive-motor interference', dual-task is typically characterized by a decline of performance compared to single-task conditions [5-9], which might be due to limitations in brain capacity allocated to perform different activities during more demanding tasks. Performance decline may also occur because the same brain structures are directly involved in the execution of the two separate tasks [5-9].

Although only some studies showed that, compared to healthy controls (HC), MS patients are characterized by higher cognitive-motor interference, the impact on daily life may be greater in them, possibly due to the need for more complex and less efficient brain network activations that may trigger fatigue [5-9]. Again, this may be particularly relevant in PMS patients since they are characterized by more severe clinical disability, brain structural damage accumulation and maladaptive functional brain network activities.

Interestingly, using functional near-infrared spectroscopy, a significant increase in prefrontal cortex activation during dual- vs single-task walking was found in MS patients [10, 11]. Compared to HC, MS patients also showed higher activation during the single-task and a

more limited increase in right premotor cortex activation moving from the single- to the dual-task [12].

Based on this background, it is tempting to speculate that the presence and severity of fatigue and the deterioration of dual-task performance in MS patients may share some common pathophysiological processes. In particular, damage in brain regions that are directly involved in fatigue as well as in motor and cognitive tasks, such as the prefrontal cortices and deep GM, may have detrimental effects for fatigue, dual-task activities and cognitive-motor interference according to the presence of fatigue [1-12]. A possible interaction between these disabling clinical features of MS is suggested by the evidence that more complex activities may increase the sense of fatigue in MS patients, and perceived fatigue may also negatively influence dual-task performances [13]. However, at present, no study explored whether specific MRI abnormalities of frontal cortical-subcortical network can contribute not only to fatigue but also to worse dual-task performance according to the presence of not of fatigue in the same cohort of MS patients.

By evaluating different MRI sequences specific to the different pathological processes of MS, in this study we investigated how the interplay between structural and functional MRI abnormalities of the frontal cortical-subcortical circuit involving the thalami, caudate nuclei and dorsolateral prefrontal cortices (DLPFC) may contribute to both fatigue and dual-task performance in PMS patients. Although damage to other brain regions, such as the parietal lobe and pallidum, may contribute to both fatigue and dual task performance, we focused on the frontal cortical-subcortical circuit since it has been consistently suggested to be associated with both fatigue and dual task performance [1-12].

Methods

Study design. This is a cross-sectional analysis, based on baseline data collected between March 2019 and August 2021 from a multicenter randomized controlled trial called "Improving Cognition in People With Progressive Multiple Sclerosis Using Aerobic Exercise and Cognitive Rehabilitation" (CogEx, identifier number: NCT03679468) [14]. For this study, 57 PMS patients enrolled in four centers participating in the MRI substudy were included: a) IRCCS San Raffaele Hospital (Milan, Italy [n=31]); b) University of Genoa (Genoa, Italy [n=18]); c) University of Alabama at Birmingham (Birmingham, Alabama, USA [n=2]) and c) Kessler Foundation (East Hanover, New Jersey, USA [n=6]).

Of note, all procedures described below were standardized across sites via comprehensive in-person and remote training, along with quality control on a case-by-case basis.

Inclusion and exclusion criteria have been previously described [14]. Briefly, to be included, MS patients had to a) have a confirmed diagnosis of PMS (primary or secondary progressive) [15]; b) be aged between 25 and 65 years old; c) have a corrected visual acuity >20/70; d) demonstrate intact language comprehension based on Token Test scores >28 (Italian for the centers of Milan and Genoa, English for the centers of Birmingham and East Hanover) and to understand instructions; e) be insufficiently active based on a Health Contribution Score of the Godin Leisure-Time Exercise Questionnaire <23 units; f) not be severely depressed based on the Beck Depression Inventory-II scores <29 [16]; g) demonstrate impaired cognitive processing speed based on Symbol Digit Modalities Test (SDMT) scores ≥1.282 standard deviation-units below the age-, sex-, and education-adjusted normative score (i.e., ≤10th percentile) [17]. Exclusion criteria were: a) wheelchair dependent (EDSS≥7.0); b) history of significant neurological or psychiatric conditions other than PMS; c) relapses or steroid use within the past 3 months; d) MRI contraindications (e.g., pacemaker,

pregnancy, breast-feeding, etc.); e) use of drugs that could affect cognition (excluding cannabis).

Ten HC, without neurologic diseases or systemic disorders potentially affecting the CNS, and with a completely normal neurologic examination, were included from IRCCS San Raffaele Hospital (Milan, Italy).

Clinical evaluation. Within three days from MRI acquisition, a neurological examination with Expanded Disability Status Scale (EDSS) score rating was performed by experienced neurologists blinded to MRI findings.

To assess fatigue, experienced evaluators administered the Modified Fatigue Impact Scale (MFIS) scale to all subjects [18]. This is a multidimensional self-report of 21 items, which examines different aspects of fatigue on everyday functioning by assessing its impact on physical, cognitive and psychosocial domains. Response options for each item range from 0 (Never) to 4 (Almost always). The global MFIS score (MFIS global) is provided by the combination of nine items for physical status (MFIS physical), 10 items for cognitive status (MFIS cognitive) and two items for psychosocial function status (MFIS psychosocial). PMS patients with an MFIS score ≥38 were considered fatigued [19].

Single-task and dual-task. Motor and cognitive performance in single-task and dual-task [5-9, 20] were evaluated (see Table 1 for a detailed description of single- and dual task paradigm). In particular, distance, speed, correct response rate during single- and dual-tasks and motor and cognitive costs during dual-task were assessed.

MRI acquisition. Using 3.0 Tesla scanners (IRCCS San Raffaele: Philips Ingenia; University of Genoa and University of Alabama: Siemens Prisma; Kessler Foundation: Siemens Skyra) and standardized procedures for subjects positioning, the following brain MRI sequences were acquired from all subjects: a) axial T2*-weighted single-shot EPI sequence for resting state (RS) fMRI; b) sagittal three-dimensional (3D) fluid-attenuated

inversion recovery (FLAIR); c) sagittal 3D T1-weighted sequence; and d) axial pulsed-gradient single-shot diffusion-weighted echo planar imaging (EPI) sequence. See supplementary methods for details regarding sequence parameters. Procedures of standardisation and quality control of MRI data have been previously described [14]. In details, before MRI scan acquisition, a mock MRI scan was performed at the four centers to evaluate image quality. Subsequently, brain MRI scans were acquired using 3.0 Tesla scanners by experienced technicians. MRI data acquired for the study were then analyzed centrally at IRCCS San Raffaele Hospital (Milan, Italy) by experienced technicians blinded to subjects' identity.

Conventional MRI analysis. Focal T2-hyperintense WM lesions were identified by a fully automated and validated approach using the 3D FLAIR and 3D T1-weighted as input images [21]. A cascade of two 3D patch-wise convolutional neural networks, already trained on manually labeled data, has been applied on the coregistered 3D FLAIR and 3D T1-weighted input images to obtain probabilistic masks for each voxel of being lesion. By thresholding voxels with ≥0.5 probability of being lesion, the final lesion mask is achieved. T2-hyperintense WM LV was obtained for each patient from their lesion masks, after a careful visual check of the results provided by the automatic segmentation.

Normalized brain volume (NBV), normalized cortical GM volume (NcGMV) and normalized WM volume (NWMV) were measured using SIENAx software using lesion-filled 3D T1-weighted sequence [22].

Volumetric analyses of thalami, caudate nuclei and DLPFC. Segmentation of the caudate nuclei and thalami was performed using the FSL FIRST tool and their volume was calculated and normalized using FSL SIENAx scaling factor (Figure 1). Among the basal ganglia, we focused on the caudate nucleus and thalamus since they have been consistently demonstrated to be involved in fatigue and dual-task performances. Conversely, we did not

include other deep GM nuclei such as the putamen and globus pallidum, that may be potentially implicated both in fatigue and dual-task performances, to limit possible collinearity among structural and functional MRI variables of structures that are anatomically and functionally strongly linked each other.

An automatic approach was used to derive a measure of DLPFC volume in each study participant. First, voxel-based morphometry (SPM12, www.fil.ion.ucl.ac.uk/spm) was run on lesion-filled 3D T1-weighted images to map differences in regional GM volumes of left and right DLPFC toward a customized atlas (see Supplementary Methods).

The segmented GM maps, transformed to the Montreal Neurological Institute space, modulated for the Jacobian of the non-linear transformation and smoothed with an 8 mm Gaussian kernel, were obtained. Then Brodmann area (BA) 9 and 46 were selected by BAs template (in which the DLPFC is contained). For each study participant, the regional GM volume in the native space was obtained by integrating the values of modulated transformed GM maps over the BA areas and then normalizing them for head size using FSL SIENAx scaling factor (Figure 1).

Diffusion tensor MRI pre-processing. Details on diffusion-weighted MRI analyses are reported in the Supplementary methods. Briefly, after motion and eddy current correction, the diffusion tensor (DT) was estimated.

Then, the spatial normalization pipeline [23] supported by the DTI-TK toolkit was applied to individual DT volumes to produce a study specific template [24]. Finally, fractional anisotropy (FA) and mean diffusivity (MD) maps from the population specific DTI template and from the transformed individual DTI were derived.

Transcallosal fibers connecting left and right DLPFC and WM tracts connecting ipsilateral thalamus, caudate nucleus and DLPFC were reconstructed (Figure 1).

To this aim, probabilistic tractography was applied to a population template, obtained from 44 HC, not used in this study, who underwent MRI acquisitions including a high angular resolution diffusion imaging (HARDI) and multi-shell diffusion-weighted sequences that were processed with Constrained Spherical Deconvolution [25]. Thalami and caudate nuclei areas defining seeds for tractography at the GM/WM interface were the masks derived from FSL FIRST tool (Figure 1). For DLPFC, two spherical seed regions of interest with a diameter of 10 millimeter were shaped onto the BAs 46 and 9 with the coordinates of the center set at X: ±42; Y:32; Z:30, as previously suggested [26, 27] (Figure 1).

The resulting tract-maps were then skeletonized and projected back to single study participants' space using the transformations derived from TBSS: i) the skeleton voxel is back projected from its position on the skeleton; ii) this point is "inverse warped" back into the study participants' native space. Finally, average FA and MD values within tracts were calculated.

RS effective connectivity (EC) analysis. RS fMRI data were analyzed using RS EC. Compared to standard RS functional connectivity analysis, which simply describes overall functional associations between regions (or networks), EC aims at assessing causal influences that the activity of a given region exerts on another one [28], and is particularly suitable for studying in details causal information flows within specific brain circuits, as it is the case of the present study. After RS fMRI pre-processing (see Supplementary methods), RS EC analysis was performed by means of spectral dynamic causal modelling (DCM) a framework proposed by Friston et al. [29], to build EC models among brain regions using RS fMRI data, as implemented in SPM12 (http://www.fil.ion.ucl.ac.uk/spm/software/spm12/) [29].

The EC was evaluated among the previously identified ROIs (i.e., thalami, caudate nuclei and DLPFC, Figure 1). Intrinsic EC strengths between each possible pair of brain

regions belonging to each circuit were estimated using spectral DCM, as described in detail elsewhere [29, 30].

Statistical analysis. Between-group differences of demographic and clinical variables among PMS patients with and without fatigue and HC were tested by Fisher's exact and Mann-Whitney U test. Wilcoxon signed-rank test was used to evaluate dual-task motor and cognitive costs in each group.

Between-group comparisons of conventional MRI variables, volumetric, diffusivity indexes and RS EC strengths of thalami, caudate nuclei and DLPFC and their connections were assessed using age-, sex- and center-adjusted linear models. T2-hyperintense WM LVs were log-transformed. To assess the stability of the results the analysis was rerun removing center from the set of covariates. False discovery rate (FDR) (Benjamini–Hochberg procedure) correction was carried out to take into account the overall number of pairwise comparisons.

Random forest (RF) classification/regression models were grown to rank demographic, clinical, significantly altered MRI variables and center effect according to their importance in explaining the presence of fatigue, global MFIS and its subscores in all PMS patients, as well as motor and cognitive performance at single- and dual-task in PMS patients stratified according to the presence of fatigue. Specifically, for each outcome, we adopted the Boruta algorithm [31] (with 10,000 trees and 2,000 iterations) in order to select a subset of relevant features. The algorithm selects features that perform better (on the basis of a binomial test with multiple comparison adjustment) than pure randomness, by iteratively comparing variables importance metric with those of shadow attributes, created by shuffling the original ones. Features with significantly worst importance than shadow attributes are progressively removed.

The goodness of fit of a new model, trained by using only the selected predictors, was expressed by the out-of-bag (OOB) accuracy (classification) or R^2 (regression), computed on the left-out observations.

SAS release 9.4 (SAS Institute, Cary, NC) and Software R (version 4.1.1) were used for computations. P values <0.05 were deemed statistically significant.

Results

Demographic, clinical and conventional MRI findings. The final study sample included 57 patients with PMS (median age=43 years, interquartile range [IQR]=47;57; 38 women, primary progressive=11, secondary progressive=46) with median disease duration of 20.0 years (IQR=12.0;26.5) and median EDSS=6.0 (IQR=4.5;6.5) and 10 HC (median age=45.0 years [IQR=36.0;53.0]; 7 women). Thirty-seven (65%) PMS patients were fatigued.

Compared to HC, both PMS patients with and without fatigue were significantly older ($p\leq0.032$), had significantly higher MFIS physical subscore ($p\leq0.005$), lower single- and dual-task distances and speeds ($p<0.001$ for all), and lower single- and dual-task correct response rates ($p<0.001$ for all) (Table 2).

Compared to non-fatigued PMS patients, those with fatigue had significantly higher EDSS score ($p=0.048$), were more frequently secondary progressive ($p=0.004$), had significantly higher MFIS global score ($p<0.001$), higher MFIS cognitive and psychosocial subscores ($p<0.001$ for both comparisons, as expected) and lower dual-task correct response rate ($p=0.019$) (Table 2).

Motor and cognitive performance significantly declined at dual-task compared to single-task in HC and PMS patients with and without fatigue ($p\leq0.030$), except for cognitive performance in non-fatigued PMS patients ($p=0.722$). No between-group differences were detected ($p\geq0.083$) (Table 2).

Conventional MRI measures. Compared to HC (4 of them showing small aspecific micro-ischaemic WM hyperintensities), both PMS patients with and without fatigue had significantly higher T2-hyperintense WM LV, and lower NBV, NcGMV and NWMV (FDR-p<0.001 for all comparisons) (Table 2). No significant differences in global lesion and volumetric measures were found between PMS with and without fatigue (FDR-p≥0.910).

Thalamic, caudate and DLPFC findings. Compared to HC, both PMS patients with and without fatigue showed significantly lower volumes of bilateral thalami (FDR-p<0.001 for all), caudate nuclei (FDR-p<0.001 for all) and DLPFC (FDR-p≤0.004) (Table 3). Both PMS subgroups also showed significantly increased MD (FDRp≤0.001 for all) in all WM tracts analysed and decreased FA in all WM tracts analysed (FDRp≤0.001 for all), except for those connecting thalamus with DLPFC bilaterally (FDR-p≥0.263) (Table 3). No significant between-group differences in volumetric and DT MRI-derived indexes were found between PMS with and without fatigue (FDR-p≥0.246).

Compared to HC, both PMS patients with and without fatigue showed significantly higher RS EC from left to right DLPFC (FDR-p≤0.021) (Table 3 and Figure 2). PMS patients without fatigue showed also a significantly lower RS EC from right thalamus to right DLPFC (FDR-p=0.034) (Table 3 and Figure 2). Compared to non-fatigued PMS patients, those with fatigue had significantly lower RS EC from left caudate nucleus to left DLPFC (FDR-p=0.046) and higher RS EC from right thalamus to right DLPFC, not surviving FDR correction (FDR-p=0.095) (Table 3 and Figure 2).

The covariate center was not statistically significant in any of the estimated models (p≥0.277). Results of between-group comparisons did not change when center was removed from the set of covariates.

Random forest informative predictors of fatigue. Informative predictors of the presence of fatigue (relative importance [%]) (OOB accuracy=0.754) were higher EDSS score (100%) and lower RS EC from left caudate nucleus to left DLPFC (73.0%) (Table 4 and Figure 2).

Higher EDSS score (100.0%), lower FA of the WM tract connecting left caudate nucleus and left thalamus (76.6%), higher MD of the WM tract connecting right caudate nucleus and right thalamus (66.8%), and longer disease duration (46.6%) predicted a higher global MFIS score (OOB R^2=0.247) (Table 4, Figures 2 and 3).

Higher EDSS score (100.0%), lower FA of the WM tract connecting left caudate nucleus and left thalamus (76.6%), and higher RS EC from right thalamus to right DLPFC (55.7%) predicted a higher MFIS physical subscore (OOB R^2=0.282) (Table 4 and Figure 2).

Lower FA of the WM tract connecting left caudate nucleus and left thalamus (100.0%), lower RS EC from left caudate nucleus to left DLPFC (85.6%) and higher RS EC from right thalamus to right DLPFC (55.7%) predicted a higher MFIS psychosocial subscore (OOB R^2=0.226) (Table 4 and Figure 2).

Random forest informative predictors of single- and dual-task performance. In PMS without fatigue, informative predictors of lower single- and dual-task distance/speed were higher EDSS score (100.0% for both outcomes) and lower FA of the WM tract connecting left caudate nucleus and left DLPFC (36.5% and 43.5%, respectively) (OOB R^2=0.535 and 0.530, respectively) (Table 5 and Figure 2).

Lower FA of transcallosal fibers connecting left and right DLPFC (100.0%) and of the WM tract connecting left caudate nucleus and left thalamus (64.4%), lower normalized volume of right caudate nucleus (83.2%), higher RS EC from left DLPFC to right DLPFC (78.0%), higher T2-hyperintense LV (73.3%), and higher MD of transcallosal fibers connecting left and right DLPFC (72.8%) predicted lower single-task correct response rate (OOB R^2=0.248) (Table 5 and Figure 2).

Lower FA of the WM tract connecting left caudate nucleus and left thalamus (100.0%), higher MD of the WM tract connecting right caudate nucleus and right DLPFC (68.6%) and higher RS EC from left DLPFC to right DLPFC (60.4%) predicted lower dual-task correct response rate (OOB R^2=0.444) (Table 5, Figures 2 and 3).

In PMS with fatigue, higher EDSS score was the only relevant predictor of lower single-task distance/speed (100.0%, OOB R^2=0.561), whereas higher EDSS score (100.0%), higher T2-hyperintense LV (24.1%), higher MD of the WM tracts connecting left caudate nucleus and left thalamus (20.0%) and left thalamus and left DLPFC (18.7%) and lower FA of the WM tract connecting right caudate nucleus and right DLPFC (16.9%) were informative predictors of lower informative predictors of dual-task distance/speed (OOB R^2=0.426) (Table 5 and Figure 2).

Higher MD of the WM tracts connecting left DLPFC with left caudate nucleus (100.0%) and left thalamus (94.5%), right DLPFC with right caudate nucleus (66.8%) and right thalamus (54.9%), right caudate nucleus with right thalamus (44.2%), lower FA and higher MD of transcallosal fibers connecting left and right DLPFC (49.5% and 40.0%, respectively), and higher T2-hyperintense LV (24.1%) predicted lower single-task correct response rate (OOB R^2=0.475) (Table 5 and Figure 2).

Lower FA and higher MD of transcallosal fibers connecting left and right DLPFC (100.0% and 74.7%, respectively) and of the WM tract connecting left caudate nucleus and left DLPFC (38.7% and 61.4%, respectively), higher MD of the WM tracts connecting right caudate nucleus and right DLPFC (89.8%) and, bilaterally, the thalamus with ipsilateral DLPFC (left=72.2%, right=60.1%), lower RS EC from left caudate nucleus to left DLPFC (58.8%) and lower NcGMV (57.6%) were informative predictors of lower dual-task correct response rate (OOB R^2=0.377) (Table 5, Figures 2 and 3).

No significant predictor for dual-task motor and cognitive costs was found in PMS patients with or without fatigue.

Discussion

In this study, we report that a substantial proportion of PMS patients were fatigued and, independently from the presence of fatigue, had worse motor and cognitive performances in all items of single- and dual-task activities compared to HC except for dual-task motor and cognitive costs. Focusing on a well-characterized cortico-subcortical network suggested to be involved in the pathophysiology of fatigue [2-4] and contributing to dual-task performance [9-12], we found that specific structural and functional MRI abnormalities were associated with fatigue impact and its severity. Moreover, they were also informative predictors of motor and cognitive performance of single- and dual-task with some differences according to the presence of fatigue. Of note, in PMS without fatigue structural and functional MRI abnormalities of the investigated frontal cortico-subcortical circuits that predicted single- and dual-task performances were more limited and mainly involved the left (dominant) hemisphere, transcallosal connections and RC EF from left to right DLFPC. Conversely, in PMS with fatigue, several and more bilateral structural MRI abnormalities of frontal cortical-subcortical networks were informative predictors of single- and dual-task performances.

The high proportion of PMS with fatigue in our study (37/57, 65%) and the significantly higher scores not only of global MFIS but also of its sub-scales in PMS compared to HC support the notion that fatigue, not only physical, but also cognitive and psychosocial, is a frequent symptom in PMS [32].

Interestingly, PMS patients showed also significantly worse motor and cognitive performance during the respective single- and dual-task conditions [5-9] compared to HC,

also in the absence of fatigue, even though PMS with fatigue showed lower dual-task correct response rate compared to those without fatigue.

Conversely, motor and cognitive performances significantly declined at dual-task compared to single-task in HC and PMS patients, with no difference in the motor and cognitive dual-task costs being found among PMS patients' subgroups and HC. Although the small sample size of HC could explain the lack of significant differences, similar dual-task costs could have been expected based on previous studies [8]. Moreover, motor and cognitive performances of PMS patients were already substantially compromised at single-task, thus it is likely that during the dual-task condition only a further limited worsening may be observed. Despite this, it is likely that the impact of the same percentage decline of performance has more detrimental impact on functioning in more disabled PMS patients.

To study the anatomical and functional correlates of fatigue and of dual-task performance in PMS patients according to the presence of fatigue, we selected a subset of brain areas (i.e., thalamus, caudate nuclei and DLPFC) and their connections which have been suggested to be consistently involved with these clinical end-points by several previous studies [2-4, 10-12, 26, 27, 33-43].

As expected, PMS patients showed significant atrophy of all GM structures investigated as well as microstructural abnormalities (in terms of decreased FA and increased MD) of the majority of the WM tracts connecting these areas.

For the analysis of fMRI alterations, we applied RS EC since it provides a potentially more direct representation of brain function and information integration between regions compared to simple functional connectivity analysis [44], allowing to investigate how one region influences another region in the brain. Interestingly, such an analysis disclosed only limited between-group RS EC differences. Compared to HC, both PMS patients with and

without fatigue had significantly higher RS EC from left to right DLPFC, with PMS patients without fatigue having also a significantly lower RS EC from right thalamus to right DLPFC.

When we explored the possible predictors of fatigue, we found that, in addition to higher EDSS score, a significantly lower RS EC from left caudate nucleus to left DLPFC was the only informative MRI measures able to explain the presence of fatigue. Our results are in line with previous studies suggesting a more prominent role of functional network abnormalities in explaining fatigue in MS patients [2-4].

Interestingly, no differences in the investigated anatomical network were found between fatigued and non-fatigued MS patients and no structural MRI measure predicted the presence of fatigue. Although apparently in contrast with previous findings [1-4], other studies did not support the associations between structural damage of frontal cortico-subcortical circuit and fatigue [1-4]. Heterogeneities in the cohorts of MS patients evaluated in terms of clinical phenotypes (i.e., relapsing-remitting or PMS), disease duration and disability, in the criteria used to define fatigue and in the MRI analyses performed may contribute to explain discrepancies among studies. In particular, while significant associations have been typically found in relapsing-remitting MS patients [2-4], different pathological processes and a plateau effect of structural brain damage may be present in PMS, thus limiting the associations between the presence of fatigue and structural MRI measures in this more severe form of the disease.

However, it should be mentioned that microstructural abnormalities of the WM tracts connecting bilateral caudate nuclei and thalami, together with abnormal RS EC from deep GM nuclei to DLPFC, were informative predictor of global MFIS and its subscores. Accordingly, both structural damage of deep GM and functional maladaptive RS EC abnormalities in the afferent connections from thalami and caudate nuclei to DLPFC may contribute to explain the severity of fatigue impact in MS patients [26, 33-36, 38-40, 45].

When we explored the possible predictors of single- and dual task performances in PMS patients stratified according to the presence of fatigue, we found that higher EDSS score and microstructural abnormalities of WM tracts connecting caudate nuclei, thalami and DLPFC were informative variables of single- and dual task distance/speed for both PMS patients' groups. Of note, the number of relevant predictors for PMS with fatigue was higher and included also higher T2-hyperintense WM LV. Our results suggest that, beside the severity of clinical disability, structural damage accumulation in clinically-relevant brain regions contributes to worse single- and dual-task motor performance, especially in the presence of fatigue.

Several MRI variables of structural damage of frontal cortico-subcortical circuit were informative predictors of single- and dual-task cognitive performance. The structural correlates of single- and dual-task impairment in MS have been only partially investigated. Focal WM lesions in the corona radiata were found to be significantly associated with dual-task cost during a combined cognitive-postural task [46]. Our study shows that several additional pathophysiological processes may negatively impact dual-task performance. Focal lesions but also microstructural abnormalities in the WM tract connecting the caudate nuclei, thalami and DLPFC may determine a disconnection syndrome among GM regions involved in motor and cognitive tasks. In addition, atrophy of strategic GM regions, such as the caudate nucleus and the cortex may explain not only more severe clinical disability and cognitive impairment, but also a lower dual-task cognitive performance.

Interestingly, while for PMS without fatigue the number of informative MRI predictors was more limited and mainly involving the left (dominant) hemisphere, a higher number of MRI variables, involving more widely also the non-dominant (right) hemisphere and transcallosal fibers, explained single- and dual-task cognitive performance in PMS with fatigue.

The presence of fatigue may be associated with more diffuse abnormalities of cortico-subcortical networks, also involving inter-hemispheric connections, that may have more substantial detrimental effects on single- and dual-task performance especially during and after demanding tasks [34, 39, 47-49].

Conversely, the contribution of fMRI abnormalities was quite limited in explaining motor and cognitive performances. In details, higher RS EC from left DLPFC to right DLPFC predicted single- and dual-task correct response rate in PMS without fatigue, whereas lower RS EC from left caudate nucleus to left DLPFC predicted dual-task correct response rate in PMS with fatigue.

Possible heterogeneities of functional network abnormalities among PMS patients may contribute to explain the limited role of fMRI abnormalities in predicting motor and cognitive performance. However, our results suggest that PMS patients may be characterized by clinically-relevant abnormal intra- and inter-hemispheric RS EC, possibly acting in opposite directions and being slightly different according to the presence or not of fatigue.

Our findings are consistent with previous studies that explored functional changes during dual-task [10-12] and that showed a significant increase in prefrontal cortex activation during dual- vs single-walking task [10, 11], being more limited in MS patients compared to HC [12]. Moreover, they are in line with the evidence of abnormal RS functional connectivity [1, 26, 38, 40, 45], or abnormal activations during motor [1, 33, 35] or cognitive tasks [1, 34, 36, 39] in specific cortico-subcortical regions. Finally, abnormal RS EC during cognitive tasks among cognitively-relevant brain regions has been described from the earliest phases of MS [50] and in the different clinical phenotypes [51, 52]. Reduced RS EC in the afferent limb of the dorsolateral prefrontal circuit has been demonstrated to mediate the relationship between cognitive performance and structural damage of WM tracts among DLPFC, caudate, globus pallidus and thalamus [53].

This study has some limitations. We evaluated a small non-matched sample of HC who have been enrolled from a single center and were significantly younger compared to PMS patients. Despite this, it is noteworthy that we were able to detect significant abnormalities in PMS both with and without fatigue compared to HC and between PMS patients' subgroups. Although analyses have been corrected for age and center, they could represent confounding factors in the analyses. However, appropriate standardisation and quality control procedures have been set to limit heterogeneities of MRI acquisitions among centers [14]. Moreover, the covariate center was not statistically significant in any of the estimated models and results of between-group comparisons were not affected by the inclusion of covariate center in the models. Finally, center was not retained as informative predictor for the presence and severity of fatigue as well as for single- and dual-task performances in both PMS with and without fatigue in the random forest analyses.

Given the evidence of accelerated brain aging in MS, further studies with larger cohorts of HC and MS patients spanning the whole lifespan are needed to better explore how aging may influence the substrates underpinning fatigue and dual-task performances in MS. This is a cross-sectional study, which evaluated only a quite small cohort of PMS patients. However, it may be difficult to obtain comprehensive and standardized clinical, functional (i.e., including single- and dual-task performances) and MRI evaluations in PMS patients. Moreover, PMS are typically characterized by high disability levels and severe structural and functional brain abnormalities. The evaluation of a larger cohort of MS patients including the main clinical phenotypes and in a longitudinal setting may allow to better investigate the dynamics of brain cortico-subcortical structural and functional abnormalities and their interplay with different clinical outcomes, including fatigue and dual-task performance. We explored the predictors of fatigue and of single- and dual-task performances according to the presence of fatigue, but the impact of fatigability was not evaluated. To limit the number of

regions of interest explored in this study, we did not investigate the role of structural and functional abnormalities of other brain regions (e.g., the pallidum and the parietal lobe) that may contribute to the occurrence of fatigue and worse dual task performance and this should be a matter of investigation of future studies. Finally, volumes of DLPFC and deep GM have been quantified using VBM and FSL FIRST, respectively, because thalamic and caudate nucleus volume may be underestimated using VBM. Despite these different methodologies, these measures have been obtained using standardized and validated approaches, already applied in previous studies [54].

In conclusion, in PMS patients, different pathological processes occurring in frontal cortico-subcortical network, including atrophy, microstructural damage of connecting WM tracts and abnormal RS EC, contribute to the severity of fatigue. Different patterns of structural and functional frontal cortico-subcortical abnormalities contribute to worse dual-task performances in PMS according to the presence of fatigue.

Our findings further support that the investigated network may have a pathogenic role for both these clinical manifestations and it may represent a target for novel therapeutic strategies aimed at limit the detrimental effects of fatigue and worse dual-task performances.

Statements and Declarations

Ethical approval

Approval was received from the local institutional ethical standards committees on human experimentation for any experiments using human subjects. Written informed consent was obtained from all subjects prior to study participation according to the Declaration of Helsinki.

Conflicts of interests

Paolo Preziosa received speaker honoraria from Roche, Biogen, Novartis, Merck Serono, Bristol Myers Squibb and Genzyme. He has received research support from Italian Ministry of Health and Fondazione Italiana Sclerosi Multipla.
Maria Assunta Rocca received speaker honoraria from Bayer, Biogen, Bristol Myers Squibb, Celgene, Genzyme, Merck Serono, Novartis, Roche, and Teva, and receives research support from the MS Society of Canada and Fondazione Italiana Sclerosi Multipla.
Elisabetta Pagani, Paola Valsasina, Nicolò Bruschi, Alessandro Meani, Cecilia Meza, Robert W. Motl and Brian Sandroff have nothing to disclose.
Maria Pia Amato received compensation for consulting services and/or speaking activities from Bayer, Biogen Idec, Merck-Serono, Novartis, Roche, Sanofi Genzyme, and Teva Pharmaceutical Industries; and receives research support from Biogen Idec, Merck-Serono, Roche, Pharmaceutical Industries and Fondazione Italiana Sclerosi Multipla.
Giampaolo Brichetto has been awarded and receives research support from Roche, Fondazione Italiana Sclerosi Multipla, ARSEP, H2020 EU Call.
Jeremy Chataway has received support from the Efficacy and Evaluation (EME) Programme, a Medical Research Council (MRC) and National Institute for Health Research (NIHR) partnership and the Health Technology Assessment (HTA) Programme (NIHR), the UK MS Society, the US National MS Society and the Rosetrees Trust. He is supported in part by the NIHR University College London Hospitals (UCLH) Biomedical Research Centre, London, UK. He has been a local principal investigator for a trial in MS funded by the Canadian MS society. A local principal investigator for commercial trials funded by: Actelion, Novartis and Roche; and has taken part in advisory boards/consultancy for Azadyne, Janssen, Merck, NervGen, Novartis and Roche.
Nancy D. Chiaravalloti is on an Advisory Board for Akili Interactive and is a member of the Editorial Boards of Multiple Sclerosis Journal and Frontiers in NeuroTrauma.

Gary Cutter is a member of Data and Safety Monitoring Boards for Astra-Zeneca, Avexis Pharmaceuticals, Biolinerx, Brainstorm Cell Therapeutics, Bristol Meyers Squibb/Celgene, CSL Behring, Galmed Pharmaceuticals, Horizon Pharmaceuticals,Hisun Pharmaceuticals, Mapi Pharmaceuticals LTD, Merck, Merck/Pfizer, Opko Biologics, OncoImmune, Neurim, Novartis, Ophazyme, Sanofi Aventis, Reata Pharmaceuticals, Teva pharmaceuticals, VielaBio Inc, Vivus, NHLBI (Protocol Review Committee), NICHD (OPRU oversight committee). He is on Consulting or Advisory Boards for Biodelivery Sciences International, Biogen, Click Therapeutics, Genzyme, Genentech, GW Pharmaceuticals, Klein-Buendel Incorporated, Medimmune, Medday, Neurogenesis LTD, Novartis, Osmotica Pharmaceuticals, Perception Neurosciences, Recursion/Cerexis Pharmaceuticals, Roche, TG Therapeutics. Dr. Cutter is employed by the University of Alabama at Birmingham and President of Pythagoras, Inc. a private consulting company located in Birmingham AL.

Ulrik Dalgas has received research support, travel grants, and/or teaching honorary from Biogen Idec, Merck-Serono, Novartis, Bayer Schering, and Sanofi Aventis as well as honoraria from serving on scientific advisory boards of Biogen Idec and Genzyme.

John DeLuca is an Associate Editor of the Archives of Physical Medicine and Rehabilitation, and Neuropsychology Review; received compensation for consulting services and/or speaking activities from Biogen Idec, Celgene, MedRhythms, and Novartis; and receives research support from Biogen Idec, National Multiple Sclerosis Society, Consortium of Multiple Sclerosis Centers, and National Institutes of Health.

Rachel Farrell has received honoraria and served on advisory panels for Merck, TEVA, Novartis, Genzyme, GW pharma (Jazz pharmaceuticals), Allergan, Merz, Ipsen and Biogen. She is supported in part by the National Institute for Health Research, University College London Hospitals, Biomedical Research Centre, London, UK.

Peter Feys is editorial board member of NNR and MSJ, provides consultancy to NeuroCompass and was board of advisory board meetings for BIOGEN.

Jennifer Freeman has been awarded research grants from the NIHR, UK.

Matilde Inglese is Co-Editor for Controversies for Multiple Sclerosis Journal; received compensation for consulting services and/or speaking activities from Biogen Idec, Merck-Serono, Novartis, Roche, Sanofi Genzyme; and received research support from NIH, NMSS, the MS Society of Canada, the Italian Ministry of Health, Fondazione Italiana Sclerosi Multipla, H2020 EU Call.

Amber Salter receives research funding from Multiple Sclerosis Society of Canada, National Multiple Sclerosis Society, CMSC and the US Department of Defense and is a member of editorial board for Neurology.
Anthony Feinstein is on Advisory Boards for Akili Interactive and Roche, and reports grants from the MS Society of Canada, book royalties from Johns Hopkins University Press, Cambridge University Press, Amadeus Press and Glitterati Editions, and speaker's honoraria from Novartis, Biogen, Roche and Sanofi Genzyme.
Massimo Filippi is Editor-in-Chief of the Journal of Neurology, Associate Editor of Human Brain Mapping, Associate Editor of Radiology, and Associate Editor of Neurological Sciences; received compensation for consulting services and/or speaking activities from Alexion, Almirall, Bayer, Biogen, Celgene, Eli Lilly, Genzyme, Merck-Serono, Novartis, Roche, Sanofi, Takeda, and Teva Pharmaceutical Industries; and receives research support from Biogen Idec, Merck-Serono, Novartis, Roche, Teva Pharmaceutical Industries, Italian Ministry of Health, Fondazione Italiana Sclerosi Multipla, and ARiSLA (Fondazione Italiana di Ricerca per la SLA).

Funding

The author(s) disclosed receipt of the following financial support for the research, authorship, and/or publication of this article: This study was funded by a grant from the Multiple Sclerosis Society of Canada (grant no. #EGID3185) and the National MS Society.

Acknowledgments

None.

Data availability

The dataset used and analysed during the current study is available from the corresponding Author on reasonable request.

References

1. Marchesi O, Vizzino C, Filippi M, Rocca MA. Current perspectives on the diagnosis and management of fatigue in multiple sclerosis. Expert Rev Neurother. 2022;22(8):681-93.
2. Arm J, Ribbons K, Lechner-Scott J, Ramadan S. Evaluation of MS related central fatigue using MR neuroimaging methods: Scoping review. J Neurol Sci. 2019;400:52-71.
3. Bertoli M, Tecchio F. Fatigue in multiple sclerosis: Does the functional or structural damage prevail? Mult Scler. 2020;26(14):1809-15.
4. Filippi M, Preziosa P, Rocca MA. Brain mapping in multiple sclerosis: Lessons learned about the human brain. Neuroimage. 2019;190:32-45.
5. Leone C, Feys P, Moumdjian L, D'Amico E, Zappia M, Patti F. Cognitive-motor dual-task interference: A systematic review of neural correlates. Neurosci Biobehav Rev. 2017;75:348-60.
6. Postigo-Alonso B, Galvao-Carmona A, Benitez I, Conde-Gavilan C, Jover A, Molina S, et al. Cognitive-motor interference during gait in patients with Multiple Sclerosis: a mixed methods Systematic Review. Neurosci Biobehav Rev. 2018;94:126-48.
7. Wajda DA, Sosnoff JJ. Cognitive-motor interference in multiple sclerosis: a systematic review of evidence, correlates, and consequences. Biomed Res Int. 2015;2015:720856.
8. Learmonth YC, Ensari I, Motl RW. Cognitive Motor Interference in Multiple Sclerosis: Insights From a Systematic Quantitative Review. Arch Phys Med Rehabil. 2017;98(6):1229-40.
9. Veldkamp R, Goetschalckx M, Hulst HE, Nieuwboer A, Grieten K, Baert I, et al. Cognitive-motor Interference in Individuals With a Neurologic Disorder: A Systematic Review of Neural Correlates. Cogn Behav Neurol. 2021;34(2):79-95.
10. Hernandez ME, Holtzer R, Chaparro G, Jean K, Balto JM, Sandroff BM, et al. Brain activation changes during locomotion in middle-aged to older adults with multiple sclerosis. J Neurol Sci. 2016;370:277-83.
11. Chaparro G, Balto JM, Sandroff BM, Holtzer R, Izzetoglu M, Motl RW, et al. Frontal brain activation changes due to dual-tasking under partial body weight support conditions in older adults with multiple sclerosis. J Neuroeng Rehabil. 2017;14(1):65.
12. Saleh S, Sandroff BM, Vitiello T, Owoeye O, Hoxha A, Hake P, et al. The Role of Premotor Areas in Dual Tasking in Healthy Controls and Persons With Multiple Sclerosis: An fNIRS Imaging Study. Front Behav Neurosci. 2018;12:296.
13. Wolkorte R, Heersema DJ, Zijdewind I. Reduced Dual-Task Performance in MS Patients Is Further Decreased by Muscle Fatigue. Neurorehabil Neural Repair. 2015;29(5):424-35.
14. Feinstein A, Amato MP, Brichetto G, Chataway J, Chiaravalloti N, Dalgas U, et al. Study protocol: improving cognition in people with progressive multiple sclerosis: a multi-arm, randomized, blinded, sham-controlled trial of cognitive rehabilitation and aerobic exercise (COGEx). BMC Neurol. 2020;20(1):204.
15. Lublin FD, Reingold SC, Cohen JA, Cutter GR, Sorensen PS, Thompson AJ, et al. Defining the clinical course of multiple sclerosis: the 2013 revisions. Neurology. 2014;83(3):278-86.
16. Sacco R, Santangelo G, Stamenova S, Bisecco A, Bonavita S, Lavorgna L, et al. Psychometric properties and validity of Beck Depression Inventory II in multiple sclerosis. Eur J Neurol. 2016;23(4):744-50.
17. Strober L, DeLuca J, Benedict RH, Jacobs A, Cohen JA, Chiaravalloti N, et al. Symbol Digit Modalities Test: A valid clinical trial endpoint for measuring cognition in multiple sclerosis. Mult Scler. 2019;25(13):1781-90.

18. Fisk JD, Ritvo PG, Ross L, Haase DA, Marrie TJ, Schlech WF. Measuring the functional impact of fatigue: initial validation of the fatigue impact scale. Clin Infect Dis. 1994;18 Suppl 1:S79-83.
19. Flachenecker P, Kumpfel T, Kallmann B, Gottschalk M, Grauer O, Rieckmann P, et al. Fatigue in multiple sclerosis: a comparison of different rating scales and correlation to clinical parameters. Mult Scler. 2002;8(6):523-6.
20. Learmonth YC, Sandroff BM, Pilutti LA, Klaren RE, Ensari I, Riskin BJ, et al. Cognitive motor interference during walking in multiple sclerosis using an alternate-letter alphabet task. Arch Phys Med Rehabil. 2014;95(8):1498-503.
21. Valverde S, Cabezas M, Roura E, Gonzalez-Villa S, Pareto D, Vilanova JC, et al. Improving automated multiple sclerosis lesion segmentation with a cascaded 3D convolutional neural network approach. Neuroimage. 2017;155:159-68.
22. Smith SM, Jenkinson M, Woolrich MW, Beckmann CF, Behrens TE, Johansen-Berg H, et al. Advances in functional and structural MR image analysis and implementation as FSL. Neuroimage. 2004;23 Suppl 1:S208-19.
23. Zhang H, Avants BB, Yushkevich PA, Woo JH, Wang S, McCluskey LF, et al. High-dimensional spatial normalization of diffusion tensor images improves the detection of white matter differences: an example study using amyotrophic lateral sclerosis. IEEE Trans Med Imaging. 2007;26(11):1585-97.
24. Zhang H, Yushkevich PA, Rueckert D, Gee JC. Unbiased white matter atlas construction using diffusion tensor images. Med Image Comput Comput Assist Interv. 2007;10(Pt 2):211-8.
25. Jeurissen B, Tournier JD, Dhollander T, Connelly A, Sijbers J. Multi-tissue constrained spherical deconvolution for improved analysis of multi-shell diffusion MRI data. Neuroimage. 2014;103:411-26.
26. Pravata E, Zecca C, Sestieri C, Caulo M, Riccitelli GC, Rocca MA, et al. Hyperconnectivity of the dorsolateral prefrontal cortex following mental effort in multiple sclerosis patients with cognitive fatigue. Mult Scler. 2016;22(13):1665-75.
27. Jaeger S, Paul F, Scheel M, Brandt A, Heine J, Pach D, et al. Multiple sclerosis-related fatigue: Altered resting-state functional connectivity of the ventral striatum and dorsolateral prefrontal cortex. Mult Scler. 2019;25(4):554-64.
28. Friston KJ, Harrison L, Penny W. Dynamic causal modelling. Neuroimage. 2003;19(4):1273-302.
29. Friston KJ, Kahan J, Biswal B, Razi A. A DCM for resting state fMRI. Neuroimage. 2014;94:396-407.
30. Zeidman P, Jafarian A, Corbin N, Seghier ML, Razi A, Price CJ, et al. A guide to group effective connectivity analysis, part 1: First level analysis with DCM for fMRI. Neuroimage. 2019;200:174-90.
31. Kursa MB, Rudnicki WR. Feature Selection with the Boruta Package. Journal of Statistical Software. 2010;36(11):1-13.
32. Marchesi O, Vizzino C, Meani A, Conti L, Riccitelli GC, Preziosa P, et al. Fatigue in multiple sclerosis patients with different clinical phenotypes: a clinical and magnetic resonance imaging study. Eur J Neurol. 2020;27(12):2549-60.
33. Filippi M, Rocca MA, Colombo B, Falini A, Codella M, Scotti G, et al. Functional magnetic resonance imaging correlates of fatigue in multiple sclerosis. Neuroimage. 2002;15(3):559-67.
34. DeLuca J, Genova HM, Hillary FG, Wylie G. Neural correlates of cognitive fatigue in multiple sclerosis using functional MRI. J Neurol Sci. 2008;270(1-2):28-39.

35. Rocca MA, Gatti R, Agosta F, Broglia P, Rossi P, Riboldi E, et al. Influence of task complexity during coordinated hand and foot movements in MS patients with and without fatigue. A kinematic and functional MRI study. J Neurol. 2009;256(3):470-82.
36. Engstrom M, Flensner G, Landtblom AM, Ek AC, Karlsson T. Thalamo-striato-cortical determinants to fatigue in multiple sclerosis. Brain Behav. 2013;3(6):715-28.
37. Damasceno A, Damasceno BP, Cendes F. Atrophy of reward-related striatal structures in fatigued MS patients is independent of physical disability. Mult Scler. 2016;22(6):822-9.
38. Hidalgo de la Cruz M, d'Ambrosio A, Valsasina P, Pagani E, Colombo B, Rodegher M, et al. Abnormal functional connectivity of thalamic sub-regions contributes to fatigue in multiple sclerosis. Mult Scler. 2018;24(9):1183-95.
39. Genova HM, Rajagopalan V, Deluca J, Das A, Binder A, Arjunan A, et al. Examination of cognitive fatigue in multiple sclerosis using functional magnetic resonance imaging and diffusion tensor imaging. PLoS One. 2013;8(11):e78811.
40. Finke C, Schlichting J, Papazoglou S, Scheel M, Freing A, Soemmer C, et al. Altered basal ganglia functional connectivity in multiple sclerosis patients with fatigue. Mult Scler. 2015;21(7):925-34.
41. Pardini M, Bonzano L, Bergamino M, Bommarito G, Feraco P, Murugavel A, et al. Cingulum bundle alterations underlie subjective fatigue in multiple sclerosis. Mult Scler. 2015;21(4):442-7.
42. Roelcke U, Kappos L, Lechner-Scott J, Brunnschweiler H, Huber S, Ammann W, et al. Reduced glucose metabolism in the frontal cortex and basal ganglia of multiple sclerosis patients with fatigue: a 18F-fluorodeoxyglucose positron emission tomography study. Neurology. 1997;48(6):1566-71.
43. Rocca MA, Meani A, Riccitelli GC, Colombo B, Rodegher M, Falini A, et al. Abnormal adaptation over time of motor network recruitment in multiple sclerosis patients with fatigue. Mult Scler. 2016;22(9):1144-53.
44. Stephan KE, Friston KJ. Analyzing effective connectivity with functional magnetic resonance imaging. Wiley Interdiscip Rev Cogn Sci. 2010;1(3):446-59.
45. Rocca MA, Valsasina P, Colombo B, Martinelli V, Filippi M. Cortico-subcortical functional connectivity modifications in fatigued multiple sclerosis patients treated with fampridine and amantadine. Eur J Neurol. 2021;28(7):2249-58.
46. Ruggieri S, Fanelli F, Castelli L, Petsas N, De Giglio L, Prosperini L. Lesion symptom map of cognitive-postural interference in multiple sclerosis. Mult Scler. 2018;24(5):653-62.
47. Tartaglia MC, Narayanan S, Arnold DL. Mental fatigue alters the pattern and increases the volume of cerebral activation required for a motor task in multiple sclerosis patients with fatigue. Eur J Neurol. 2008;15(4):413-9.
48. Chen MH, DeLuca J, Genova HM, Yao B, Wylie GR. Cognitive Fatigue Is Associated with Altered Functional Connectivity in Interoceptive and Reward Pathways in Multiple Sclerosis. Diagnostics (Basel). 2020;10(11).
49. Chen MH, Wylie GR, Sandroff BM, Dacosta-Aguayo R, DeLuca J, Genova HM. Neural mechanisms underlying state mental fatigue in multiple sclerosis: a pilot study. J Neurol. 2020;267(8):2372-82.
50. Au Duong MV, Boulanouar K, Audoin B, Treseras S, Ibarrola D, Malikova I, et al. Modulation of effective connectivity inside the working memory network in patients at the earliest stage of multiple sclerosis. NeuroImage. 2005;24(2):533-8.
51. Dobryakova E, Rocca MA, Valsasina P, Ghezzi A, Colombo B, Martinelli V, et al. Abnormalities of the executive control network in multiple sclerosis phenotypes: An fMRI effective connectivity study. Hum Brain Mapp. 2016;37(6):2293-304.

52. Dobryakova E, Rocca MA, Valsasina P, DeLuca J, Filippi M. Altered neural mechanisms of cognitive control in patients with primary progressive multiple sclerosis: An effective connectivity study. Hum Brain Mapp. 2017;38(5):2580-8.
53. Meng D, Welton T, Elsarraj A, Morgan PS, das Nair R, Constantinescu CS, et al. Dorsolateral prefrontal circuit effective connectivity mediates the relationship between white matter structure and PASAT-3 performance in multiple sclerosis. Hum Brain Mapp. 2021;42(2):495-509.
54. Cordani C, Preziosa P, Valsasina P, Meani A, Pagani E, Morozumi T, et al. MRI of Transcallosal White Matter Helps to Predict Motor Impairment in Multiple Sclerosis. Radiology. 2022;302(3):639-49.

Table 1. Details of single- and dual-task exercises and the clinical outcomes evaluated.

Task	**Definition**	
Motor task	Motor single-task was performed by standing with the toes in contact with a starting line. Then, participant had to walk at spontaneous speed for one minute in a corridor 15 or 30 metres long; the participant should quickly turn around behind the cone he finds at each end of the corridor and return without hesitation. The metres walked are calculated and then the average speed is extracted. MS Patients could use aids if necessary	
Cognitive task	Cognitive single-task was performed sitting on a chair, and reciting aloud and alternately letters of the alphabet, starting with the letter L. For example, if participant was given the letter S, he/she should say U, and then Z. When the participant has reached the end of the alphabet, he/she had to continue by starting a new round of the alphabet but keep doing it alternately. For example, after Z, participant should answer B and when he/she has got to the end they have to start again, for a total time of one minute	
Combined motor and cognitive tasks	Combined motor and cognitive dual-task was performed like the previous cognitive single-task, starting with the letter C, but instead of sitting on the chair while reciting the alternating letters, the participant had to walk as explained above in the motor test. Thus, performing the two tasks at the same time	
Outcome	**Definition**	**Interpretation**
Single-task distance	Meters walked in 60 seconds	Lower score: lower performance
Dual-task distance	Meters walked in 60 seconds while performing the alternating alphabet task	Lower score: lower performance
Single-task speed	Speed obtained in walking for 60 seconds $\frac{\text{meters walked during single motor task}}{\text{60 seconds}}$	Lower score: lower performance

Dual-task speed	Speed obtained in walking for 60 seconds while performing the alternating alphabet task $\frac{\text{meters walked during dual} - \text{task}}{60 \text{ seconds}}$	Lower score: lower performance
Single-task correct response rate	The number of correct answers and the number of totally given answers within 60 seconds. From this the correct response rate is calculated according to formula: $\frac{\text{correct answers during single} - \text{task}}{60 \text{ seconds}} \times 100$	Lower score: lower performance
Dual-task correct response rate	The number of correct answers and the number of totally given answers within 60 seconds. From this the correct response rate is calculated according to formula: $\frac{\text{correct answers during dual} - \text{task}}{60 \text{ seconds}} \times 100$	Lower score: lower performance
Dual-task motor cost	Motor cost of the dual-task compared to the single task, calculated according to the formula $\frac{(\text{single} - \text{task speed}) - (\text{dual} - \text{task speed})}{\text{single} - \text{task speed}} \times 100$	Higher score: lower motor performance in dual-task
Dual-task cognitive cost	Cognitive cost of the dual-task compared to the single task, calculated according to the formula: $\frac{(\text{single} - \text{task correct response rate}) - (\text{dual} - \text{task correct response rate})}{\text{single} - \text{task correct response rate}} \times 100$	Higher score: lower cognitive performance in dual-task

Table 2. Main demographic and clinical variables evaluated in HC and in MS patients as a whole and according to the presence of fatigue.

Variable	**HC (n=10)**	**nF PMS (n=20)**	**F PMS (n=37)**	**p value nF PMS *vs* HC**	**p value F PMS *vs* HC**	**p value F PMS *vs* nF PMS**
Median age (IQR) [years]	45.0 (36.0;53.0)	51.5 (47.0;56.5)	53.0 (48.0;57.0)	0.032	0.012	0.530
Men (%) Women (%)	3 (30%) 7 (70%)	9 (45%) 11 (55%)	10 (27%) 27 (73%)	0.694a	0.999a	0.240a
Median EDSS (IQR)	-	5.5 (3.5;6.5)	6.5 (5.0;6.5)	-	-	**0.048**
Median disease duration (IQR) [years]	-	18.5 (4.2;28.5)	21.0 (13.5;26.0)	-	-	0.273
PMS phenotype (primary/secondary)	-	8/12	3/34	-	-	**0.011a**
Median MFIS global (IQR)	16 (5;27)	27 (22;32)	51 (44;60)	0.052	**<0.001**	**<0.001**
Median MFIS physical (IQR)	3.5 (0;11)	14 (10.5;19)	26 (23;29)	**0.005**	**<0.001**	**<0.001**
Median MFIS cognitive (IQR)	11.5 (5;12)	9 (4.5;12)	23 (17;27)	0.427	**<0.001**	**<0.001**
Median MFIS psychosocial (IQR)	1 (0;2)	2 (1.5;3)	5 (4;6)	0.065	**<0.001**	**<0.001**
Median single-task distance (IQR) [m]	76.5 (75;78)	45.5 (31.5;55.5)	31 (20;50)	**<0.001**	**<0.001**	0.093
Median single-task speed (IQR) [m/s]	1.3 (1.2;1.3)	0.8 (0.5;0.9)	0.5 (0.3;0.8)			
Median dual-task distance (IQR) [m]	61 (60;67)	40.5 (25.5;48)	28 (17;40)	**<0.001**	**<0.001**	0.086
Median dual-task speed (IQR) [m/s]	1.0 (1.0;1.1)	0.7 (0.4;0.8)	0.5 (0.3;0.7)			
Median single-task correct response rate (IQR)	76.7 (70.4;85.0)	45.8 (38.3;61.7)	40.0 (26.7;50.0)	**<0.001**	**<0.001**	0.096

Median dual-task correct response rate (IQR)	73.3 (65.0;85.0)	45.8 (32.5;63.3)	36.7 (26.7;45.0)	**0.002**	**<0.001**	**0.019**
Median dual-task motor cost (IQR)	21.5 (8.0;32.7)	12.6 (8.6;18.9)	10.5 (2.6;24.1)	0.153 [**0.002b**]	0.083 [<**0.001b**]	0.575 [<**0.001b**]
Median dual-task cognitive cost (IQR)	4.6 (2.0;7.0)	-2.4 (-16.2;16.4)	8.3 (-3.6;25.0)	0.226 [**0.008b**]	0.541 [0.722b]	0.116 [**0.030b**]

Between-group comparisons p value analyses were obtained using Mann-Whitney test unless otherwise specified: a=Fisher's exact test; b=Wilcoxon signed-rank test.

°Comparison performed on log-scale.

Statistically significant comparisons are highlighted in bold.

Abbreviations: EDSS=Expanded Disability Status Scale; F=fatigued; HC=healthy controls; IQR=interquartile range; MFIS=modified fatigue impact scale; m=meter; nF=non-fatigued; s=second; PMS=progressive multiple sclerosis.

Table 3. Comparisons of global lesional and volumetric measures and of thalamic, caudate nuclei and DLPFC volumes, DT MRI measures of their connecting WM tracts and RS EC measures among these regions between HC and MS patients according to the presence of fatigue (age-, sex- and center-adjusted linear models).

Variable	**HC**	**PMS patients**		**nF PMS *vs* HC**		**F PMS *vs* HC**		**F PMS *vs* nF PMS**	
		F	**nF**						
	EM (SE)	**EM (SE)**	**EM (SE)**	**EMD (95% CI)**	**p (FDR-p)**	**EMD (95% CI)**	**p (FDR-p)**	**EMD (95% CI)**	**p (FDR-p)**
Volumetric measures									
T2-hyperintense WM LV[a] [median (IQR)]	1.16 (0.41) [0.00 (0.00;0.21)]	3.92 (0.15) [7.89 (5.28;13.15)]	3.86 (0.13) [7.47 (4.41;20.51)]	2.76 (1.83;3.68)	**<0.001 (<0.001)**	2.70 (1.78;3.63)	**<0.001 (<0.001)**	-0.05 (-0.33;0.23)	0.702 (0.910)
NBV	1610 (18)	1485 (17)	1490 (14)	-125 (-161;-89)	**<0.001 (<0.001)**	-120 (-154;-85)	**<0.001 (<0.001)**	5 (-27;38)	0.737 (0.910)
NcGMV	666 (13)	610 (12)	612 (9)	-55 (-82;-28)	**<0.001 (0.001)**	-53 (-79;-27)	**<0.001 (0.001)**	2 (-20;24)	0.840 (0.912)
NWMV	717 (9)	674 (9)	676 (7)	-43 (-63;-23)	**<0.001 (<0.001)**	-41 (-59;-23)	**<0.001 (<0.001)**	2 (-14;18)	0.800 (0.912)
Normalized volume — L thalamus	12.30 (0.41)	9.88 (0.35)	9.93 (0.31)	-2.41 (-3.19;-1.64)	**<0.001 (<0.001)**	-2.37 (-3.17;-1.56)	**<0.001 (<0.001)**	0.05 (-0.57;0.67)	0.877 (0.917)

	R thalamus	11.80 (0.40)	9.51 (0.37)	9.41 (0.34)	-2.29 (-2.95;-1.62)	**<0.001 (<0.001)**	-2.39 (-3.12;-1.66)	**<0.001 (<0.001)**	-0.11 (-0.77;0.55)	0.749 (0.910)
	L caudate nucleus	4.99 (0.21)	4.21 (0.21)	4.21 (0.19)	-0.78 (-1.12;-0.45)	**<0.001 (<0.001)**	-0.78 (-1.15;-0.42)	**<0.001 (<0.001)**	-0.00 (-0.37;0.37)	0.999 (0.999)
	R caudate nucleus	5.08 (0.21)	4.27 (0.21)	4.25 (0.17)	-0.81 (-1.22;-0.40)	**<0.001 (0.001)**	-0.82 (-1.21;-0.43)	**<0.001 (<0.001)**	-0.01 (-0.39;0.37)	0.949 (0.958)
	L DLPFC	15.13 (0.53)	13.04 (0.43)	13.18 (0.35)	-2.09 (-3.23;-0.95)	**0.001 (0.003)**	-1.95 (-3.06;-0.84)	**0.001 (0.004)**	0.14 (-0.64;0.92)	0.719 (0.910)
	R DLPFC	16.39 (0.53)	13.61 (0.44)	13.55 (0.34)	-2.78 (-3.95;-1.61)	**<0.001 (<0.001)**	-2.84 (-3.95;-1.74)	**<0.001 (<0.001)**	-0.06 (-0.87;0.74)	0.874 (0.917)
DT MRI measures										
FA	DLPFC transcallosal	0.34 (0.01)	0.29 (0.01)	0.29 (0.01)	-0.05 (-0.08;-0.03)	**<0.001 (0.001)**	-0.05 (-0.08;-0.03)	**<0.001 (0.001)**	0.00 (-0.02;0.02)	0.815 (0.912)
	L caudate nucleus - L DLPFC	0.31 (0.01)	0.28 (0.01)	0.27 (0.01)	-0.03 (-0.05;-0.01)	**0.001 (0.003)**	-0.04 (-0.07;-0.02)	**<0.001 (<0.001)**	-0.01 (-0.04;0.02)	0.394 (0.583)
	L caudate nucleus - L thalamus	0.30 (0.01)	0.28 (0.01)	0.27 (0.01)	-0.02 (-0.04;-0.01)	**0.001 (0.003)**	-0.03 (-0.05;-0.02)	**<0.001 (<0.001)**	-0.01 (-0.02;0.00)	0.199 (0.355)
	L thalamus - L DLPFC	0.32 (0.01)	0.32 (0.01)	0.31 (0.01)	-0.00 (-0.02;0.01)	0.785 (0.912)	-0.01 (-0.03;0.01)	0.169 (0.311)	-0.01 (-0.02;0.00)	0.110 (0.246)
	R caudate nucleus - R DLPFC	0.30 (0.01)	0.26 (0.01)	0.26 (0.01)	-0.04 (-0.06;-0.03)	**<0.001 (<0.001)**	-0.05 (-0.06;-0.03)	**<0.001 (<0.001)**	-0.00 (-0.02;0.02)	0.870 (0.917)

	R caudate nucleus - R thalamus	0.30 (0.01)	0.26 (0.01)	0.26 (0.01)	-0.03 (-0.05;-0.02)	**<0.001 (<0.001)**	-0.04 (-0.05;-0.02)	**<0.001 (<0.001)**	-0.00 (-0.01;0.01)	0.557 (0.780)
	R thalamus - R DLPFC	0.33 (0.01)	0.33 (0.01)	0.32 (0.01)	-0.00 (-0.01;0.01)	0.795 (0.912)	-0.01 (-0.02;0.00)	0.128 (0.263)	-0.01 (-0.02;0.00)	0.094 (0.215)
MD	DLPFC transcallosal	0.87 (0.05)	1.08 (0.05)	1.09 (0.04)	0.21 (0.13;0.28)	**<0.001 (<0.001)**	0.21 (0.12;0.30)	**<0.001 (<0.001)**	0.00 (-0.08;0.09)	0.916 (0.949)
	L caudate nucleus - L DLPFC	0.71 (0.09)	1.12 (0.10)	1.15 (0.08)	0.41 (0.24;0.57)	**<0.001 (<0.001)**	0.44 (0.29;0.59)	**<0.001 (<0.001)**	0.03 (-0.16;0.22)	0.745 (0.910)
	L caudate nucleus - L thalamus	0.74 (0.05)	1.01 (0.05)	1.03 (0.04)	0.27 (0.19;0.35)	**<0.001 (<0.001)**	0.28 (0.21;0.36)	**<0.001 (<0.001)**	0.02 (-0.08;0.11)	0.736 (0.910)
	L thalamus - L DLPFC	0.70 (0.036)	0.85 (0.04)	0.87 (0.03)	0.15 (0.10;0.21)	**<0.001 (<0.001)**	0.17 (0.11;0.23)	**<0.001 (<0.001)**	0.02 (-0.05;0.09)	0.561 (0.780)
	R caudate nucleus - R DLPFC	0.76 (0.07)	1.04 (0.08)	1.10 (0.07)	0.28 (0.17;0.38)	**<0.001 (<0.001)**	0.33 (0.21;0.46)	**<0.001 (<0.001)**	0.06 (-0.08;0.19)	0.411 (0.596)
	R caudate nucleus - R thalamus	0.74 (0.05)	1.08 (0.05)	1.09 (0.04)	0.34 (0.25;0.425)	**<0.001 (<0.001)**	0.35 (0.26;0.43)	**<0.001 (<0.001)**	0.01 (-0.09;0.11)	0.821 (0.912)
	R thalamus - R DLPFC	0.68 (0.03)	0.82 (0.03)	0.85 (0.03)	0.14 (0.10;0.18)	**<0.001 (<0.001)**	0.17 (0.11;0.23)	**<0.001 (<0.001)**	0.03 (-0.03;0.09)	0.321 (0.495)
fMRI measures										
RS EC	L DLPFC - R DPLFC	-0.14 (0.08)	0.16 (0.07)	0.09 (0.06)	0.30 (0.13;0.47)	**0.001 (0.004)**	0.23 (0.07;0.39)	**0.008 (0.021)**	-0.07 (-0.20;0.06)	0.301 (0.470)

	R DLPFC - L DLPFC	0.21 (0.11)	0.03 (0.10)	-0.01 (0.07)	-0.18 (-0.42;0.07)	0.154 (0.300)	-0.22 (-0.44;-0.01)	0.045 (0.104)	-0.05 (-0.25;0.15)	0.634 (0.850)
	L caudate nucleus - L thalamus	0.02 (0.14)	-0.03 (0.08)	-0.01 (0.07)	-0.04 (-0.36;0.27)	0.770 (0.912)	-0.03 (-0.34;0.28)	0.839 (0.912)	0.01 (-0.13;0.16)	0.857 (0.917)
	L thalamus - L caudate nucleus	0.13 (0.14)	-0.11 (0.12)	-0.03 (0.08)	-0.24 (-0.57;0.09)	0.155 (0.300)	-0.16 (-0.45;0.14)	0.280 (0.443)	0.08 (-0.16;0.31)	0.496 (0.707)
	R caudate nucleus - R thalamus	-0.12 (0.12)	0.06 (0.08)	0.05 (0.07)	0.18 (-0.08;0.45)	0.164 (0.307)	0.17 (-0.10;0.43)	0.199 (0.355)	-0.01 (-0.15;0.12)	0.838 (0.912)
	R thalamus - R caudate nucleus	-0.01 (0.19)	0.08 (0.11)	-0.08 (0.08)	0.09 (-0.34;0.52)	0.667 (0.884)	-0.06 (-0.48;0.35)	0.750 (0.910)	-0.15 (-0.36;0.05)	0.137 (0.275)
	L caudate nucleus - L DLPFC	-0.12 (0.23)	0.10 (0.13)	-0.18 (0.10)	0.22 (-0.29;0.72)	0.375 (0.569)	-0.06 (-0.56;0.43)	0.788 (0.912)	-0.28 (-0.51;-0.05)	**0.019 (0.046)**
	L DLPFC - L caudate nucleus	-0.09 (0.11)	0.01 (0.08)	-0.08 (0.07)	0.10 (-0.13;0.33)	0.390 (0.583)	0.01 (-0.22;0.24)	0.942 (0.958)	-0.09 (-0.24;0.06)	0.233 (0.387)
	R caudate nucleus - R DLPFC	0.25 (0.16)	-0.00 (0.08)	0.05 (0.08)	-0.26 (-0.59;0.07)	0.115 (0.252)	-0.20 (-0.53;0.14)	0.225 (0.387)	0.06 (-0.08;0.20)	0.413 (0.596)
	R DLPFC - R caudate nucleus	0.13 (0.13)	-0.03 (0.08)	-0.06 (0.08)	-0.15 (-0.41;0.10)	0.227 (0.387)	-0.19 (-0.46;0.08)	0.160 (0.305)	-0.04 (-0.18;0.11)	0.619 (0.840)
	L thalamus - L DLPFC	-0.15 (0.18)	0.08 (0.12)	0.06 (0.10)	0.23 (-0.15;0.61)	0.239 (0.387)	0.20 (-0.18;0.59)	0.277 (0.443)	-0.02 (-0.23;0.19)	0.831 (0.912)
	L DLPFC -	0.11	0.06	-0.04	-0.05	0.699	-0.15	0.234	-0.10	0.119

	L thalamus	(0.12)	(0.07)	(0.06)	(-0.30;0.21)	(0.910)	(-0.40;0.10)	(0.387)	(-0.23;0.03)	(0.256)
	R thalamus - R DLPFC	0.37 (0.16)	-0.09 (0.10)	0.11 (0.09)	-0.46 (-0.81;-0.11)	**0.013 (0.034)**	-0.265 (-0.615;0.085)	0.129 (0.263)	0.195 (0.009;0.380)	**0.040** (0.095)
	R DLPFC - R thalamus	0.01 (0.15)	0.02 (0.09)	-0.07 (0.09)	0.01 (-0.30;0.32)	0.941 (0.958)	-0.08 (-0.40;0.24)	0.600 (0.824)	-0.09 (-0.26;0.07)	0.257 (0.419)

a=Analyses performed on log-scale.

Statistically significant comparisons are highlighted in bold.

Abbreviations: CI=confidence interval; DLPFC=dorsolateral prefrontal cortex; DT=diffusion tensor; EM=estimated mean; EMD=estimated mean difference; F=fatigued; FA=fractional anisotropy; FDR=false discovery rate; HC=healthy controls; IQR=interquartile range; L=left; LV=lesion volume; MD=mean diffusivity; MRI=magnetic resonance imaging; NBV=normalized brain volume; NcGMV=normalized cortical gray matter volume; nF=non-fatigued; NWMV=normalized white matter volume; PMS=progressive multiple sclerosis; R=right; RS EC=resting state effective connectivity; SE=standard error; WM=white matter.

Volumetric measures are expressed in units of milliliter; MD is expressed in units of $mm^2/sec \times 10^{-3}$; RS EC is expressed in Hertz (1/sec); FA is a dimensionless index.

Table 4. Random forest informative predictors of fatigue in PMS patients. Demographic, clinical and MRI features selected by Boruta algorithm as relevant predictors of the presence of fatigue, global MFIS and its subscores in PMS patients are listed. Median importance of each predictor, achieved across iterations, the relative importance, and the performance of a final random forest model including only selected variables are also reported.

Outcome	**Predictor**	**Median importance (IQR)**	**RI**	**OOB accuracy**
F PMS vs nF PMS	EDSS score	39.6 (24.8;43.1)	100.0	0.754
	RS EC L caudate nucleus - L DLPFC	28.9 (18.3;36.2)	73.0	
Outcome	**Predictor**	**Median importance (IQR)**	**RI**	**OOB R^2**
MFIS global	EDSS score	31.2 (28.6;33.9)	100.0	0.247
	FA L caudate nucleus - L thalamus	23.9 (21.4;26.5)	76.6	
	MD R caudate nucleus - R thalamus	20.9 (19;23.2)	66.8	
	Disease duration	14.6 (11.2;17.6)	46.6	
MFIS physical	EDSS score	31.3 (26.3;34.3)	100.0	0.282
	FA L caudate nucleus - L thalamus	22.4 (19.3;25)	71.5	
	RS EC R thalamus - R DLPFC	17.5 (14;20.1)	55.7	
MFIS psychosocial	FA L caudate nucleus - L thalamus	28.3 (23.9;30.3)	100.0	0.226
	RS EC L caudate nucleus - L DLPFC	24.3 (20.7;28.2)	85.6	
	RS EC R thalamus - R DLPFC	21.2 (13.8;24.9)	74.9	

Abbreviations: DLPFC=dorsolateral prefrontal cortex; EDSS=Expanded Disability Status Scale; FA=fractional anisotropy; IQR=interquartile range; L=left; MD=mean diffusivity; MFIS=modified fatigue impact scale; MRI=magnetic resonance imaging; OOB=out-of-bag; R=right; RI=relative importance; RS EC=resting state effective connectivity.

Volumetric measures are expressed in units of milliliter; MD is expressed in units of $mm^2/sec \times 10^{-3}$; RS EC is expressed in Hertz (1/sec); FA is a dimensionless index.

Table 5. Random forest informative predictors of single- and dual-task performance in PMS patients. Demographic, clinical and MRI features selected by Boruta algorithm as relevant predictors of single- and dual-task performance in PMS patients, stratified according to the presence of fatigue, are listed. Median importance of each predictor, achieved across iterations, the relative importance, and the performance of a final random forest model including only selected variables are also reported.

Outcome	nF PMS				F PMS			
	Predictor	**Median importance (IQR)**	**RI**	**OOB R^2**	**Predictor**	**Median importance (IQR)**	**RI**	**OOB R^2**
Single-task distance/speed	EDSS score	56.0 (53.2;58.1)	100.0	0.535	EDSS score	51.5 (50.6;52.3)	100.0	0.561
	FA L caudate nucleus - L DLPFC	20.5 (16.9;22.7)	36.5					
Dual-task distance/speed	EDSS score	51.8 (49.1;55.1)	100.0	0.530	EDSS score	86.1 (83.9;87.6)	100.0	0.426
	FA L caudate nucleus - L DLPFC	22.5 (20.6;24)	43.5		T2-hyperintense WM LV[a]	20.7 (19.5;22.5)	24.1	
					MD L caudate nucleus - L thalamus	17.2 (15.4;18.9)	20.0	
					MD L thalamus - L DLPFC	16.1 (14.8;18)	18.7	
					FA R caudate nucleus - R DLPFC	14.6 (12.6;16.2)	16.9	
Single-task correct response rate	FA DLPFC transcallosal	18 (16.9;19.2)	100.0	0.248	MD L caudate nucleus - L DLPFC	45.2 (42.6;46.1)	100.0	0.475
	Normalized R caudate nucleus volume	15 (12.9;17)	83.2		MD L thalamus - L DLPFC	42.7 (40.7;43.7)	94.5	
	RS EC L DLPFC - R DPLFC	14 (12.8;15.2)	78.0		MD R caudate nucleus - R DLPFC	30.2 (29.4;30.8)	66.8	
	T2-hyperintense WM LV[a]	13.2 (12;14.6)	73.3		MD R thalamus - R DLPFC	24.8 (24.3;25.4)	54.9	
	MD DLPFC transcallosal	13.1 (11.6;14.5)	72.8		FA DLPFC transcallosal	22.4 (21.5;23.4)	49.5	
	FA L caudate nucleus - L thalamus	11.6 (10.4;13)	64.4		MD R caudate nucleus - R thalamus	20.0 (19.2;20.9)	44.2	

					MD DLPFC transcallosal	18.1 (17.1;18.9)	40.0	
					T2-hyperintense WM LV[a]	14.1 12.9;15.2)	31.3	
Dual-task correct response rate	FA L caudate nucleus - L thalamus	28.1 (25.6;30.2)	100.0	0.444	FA DLPFC transcallosal	32.1 (30.7;33.3)	100.0	0.377
	MD R caudate nucleus - R DLPFC	19.3 (17;22)	68.6		MD R caudate nucleus - R DLPFC	28.8 (27.7;29.9)	89.8	
	RS EC L DLPFC - R DPLFC	17 (14.9;19.2)	60.4		MD DLPFC transcallosal	23.9 (22.6;24.8)	74.7	
					MD L thalamus - L DLPFC	23.2 (22.1;24)	72.2	
					MD L caudate nucleus - L DLPFC	19.7 (18.6;20.8)	61.4	
					MD R thalamus - R DLPFC	19.3 (18.4;20.2)	60.1	
					RS EC L caudate nucleus - L DLPFC	18.9 17.1;20.2)	58.8	
					NcGMV	18.5 (16.8;19.5)	57.6	
					FA L caudate nucleus - L DLPFC	12.4 (11.3;13.5)	38.7	

Abbreviations: DLPFC=dorsolateral prefrontal cortex; EDSS=Expanded Disability Status Scale; F=fatigued; FA=fractional anisotropy; IQR=interquartile range; L=left; LV=lesion volume; MD=mean diffusivity; MRI=magnetic resonance imaging; NcGMV=normalized cortical gray matter volume; nF=non-fatigued; OOB=out-of-bag; PMS=progressive multiple sclerosis; R=right; RI=relative importance; RS EC=resting state effective connectivity; WM=white matter.

Figure legends

Figure 1. Selected deep gray matter and cortical regions, reconstructed white matter tracts and *a priori* selected ROIs for RS EC analysis. Map of the thalami, caudate nuclei and DLPFC selected as ROIs and representation of the reconstructed white matter tracts connecting these regions. (A) Regions of interest: left thalamus (encoded in blue), right thalamus (encoded in light blue), left caudate nucleus (encoded in fuchsia), right caudate nucleus (encoded in yellow), left DLFC (encoded in red), right DLPFC (encoded in green). The thalami and caudate nuclei were segmented using FIRST, whereas region of interest of DLPFC was built by placing spheres with a 10-millimeter diameter centered on ±42, +30, +32 MNI coordinates. Reconstructed white matter tracts on fractional anisotropy template: (B) WM fibers connecting left caudate nucleus and left thalamus; (C WM fibers connecting left caudate nucleus and left DLPFC; (D) WM fibers connecting left thalamus and left DLPFC; (E) Transcallosal fibers between left DLPFC - right DLPFC; Similar WM tracts were also obtained for the right hemisphere. The color-coding indicates the local fiber orientation (red, left-right; green, dorsal-ventral; blue, cranial-caudal). (F) ROIs that were selected *a priori* for resting state effective connectivity analysis; left DLPFC (encoded in blue fuchsia), right DLPFC (encoded in pink), left caudate nucleus (encoded in green), right caudate nucleus (encoded in light blue), left thalamus (encoded in red; right thalamus is encoded in yellow. See text for further details.
Abbreviations: A=anterior; DLPFC=dorsolateral prefrontal cortex; L=left; MNI=Montreal Neurological Institute; P=posterior; R=right; ROI=region of interest; RS EC=resting state effective connectivity.

Figure 2. Significant RS EC between-group differences among PMS patients with and without fatigue and HC, and RS EC variables being relevant to explain the different clinical outcomes of the study. Significant differences in RS EC between (A) nF PMS patients compared to HC, (B) F PMS patients compared to HC, and (C) F PMS patients compared to nF PMS patients.
Continuous white arrows represent higher RS EC; dotted white arrows represent lower RS EC.
Results of the random forest analyses showing RS EC variables being selected as informative predictor of (D) MFIS physical score, (E) MFIS psychosocial, (F) single-task correct response rate in nF PMS patients, (G) dual-task correct response rate in nF PMS patients, and (H) dual-task correct response rate in F PMS patients,
Continuous orange arrows represent positive associations; dotted white arrows represent negative associations.

See text for further details.
Abbreviations: A=anterior; DLPFC=dorsolateral prefrontal cortex; F=fatigued; HC=healthy controls; L=left; MFIS=modified fatigue impact scale; nF=non-fatigued; P=posterior; PMS=progressive multiple sclerosis; R=right; RS EC=resting state effective connectivity.

Figure 3. Random forest informative predictors of MFIS score and dual task correct response rate in PMS patients according to the presence of fatigue. Distribution of **v**ariable importance, achieved across iterations of Boruta algorithm, of demographic, clinical and MRI features to explain (A) MFIS global in all PMS, dual task correct response rate in PMS (B) without and (C) with fatigue. Boruta compares the importance of the original variables with the highest feature importance of the shadow features, obtained using features permuted copies. Poorly performing variables are progressively discarded.
Selected features are shown in green, discarded features in red. Maximum, mean and minimum importance achieved by shadows attributes are shown in blue.
Abbreviations: DLPFC=dorsolateral prefrontal cortex; EDSS=Expanded Disability Status Scale; F=fatigued; FA=fractional anisotropy; L=left; MD=mean diffusivity; MFIS=modified fatigue impact scale; MRI=magnetic resonance imaging; NcGMV=normalized cortical gray matter volume; nF=non-fatigued; R=right; RS EC=resting state effective connectivity.

Figure 1:

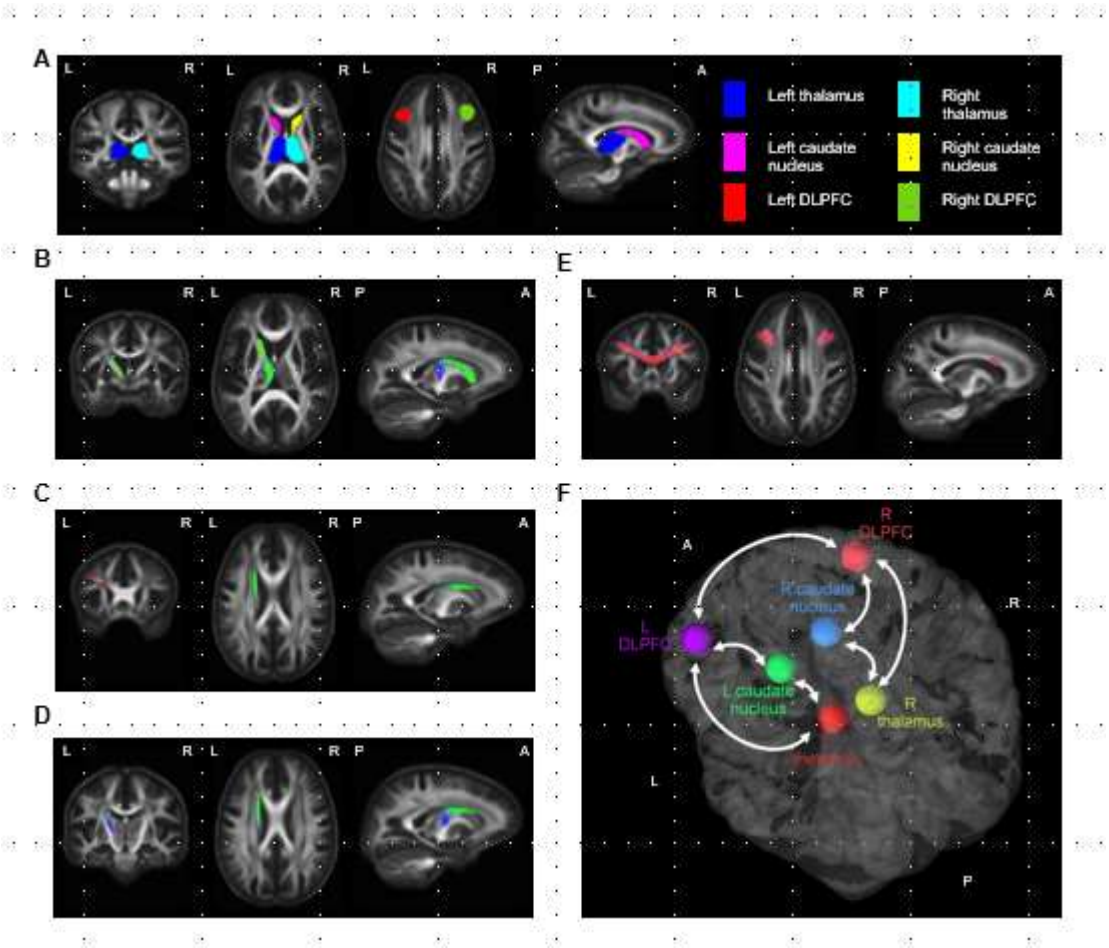
A
B
C
D
E
F
Left thalamus
Right thalamus
Left caudate nucleus
Right caudate nucleus
Left DLPFC
Right DLPFC
R DLPFC
R caudate nucleus
L DLPFC
L caudate nucleus
R thalamus

Figure 2:

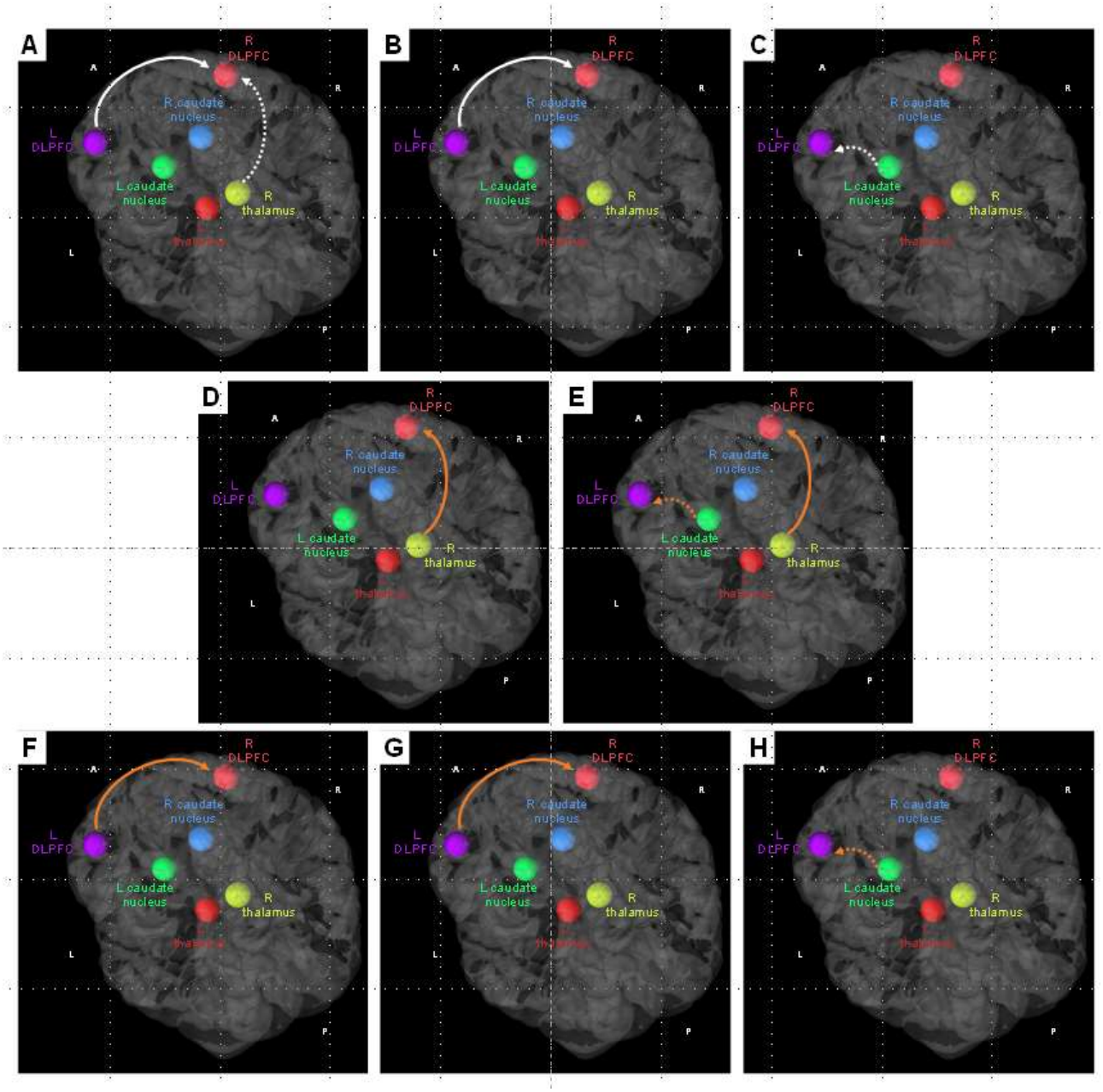
A
R DLPFC
R caudate nucleus
L DLPFC
L caudate nucleus
R thalamus
B
C
D
E
F
G
H

Figure 3:

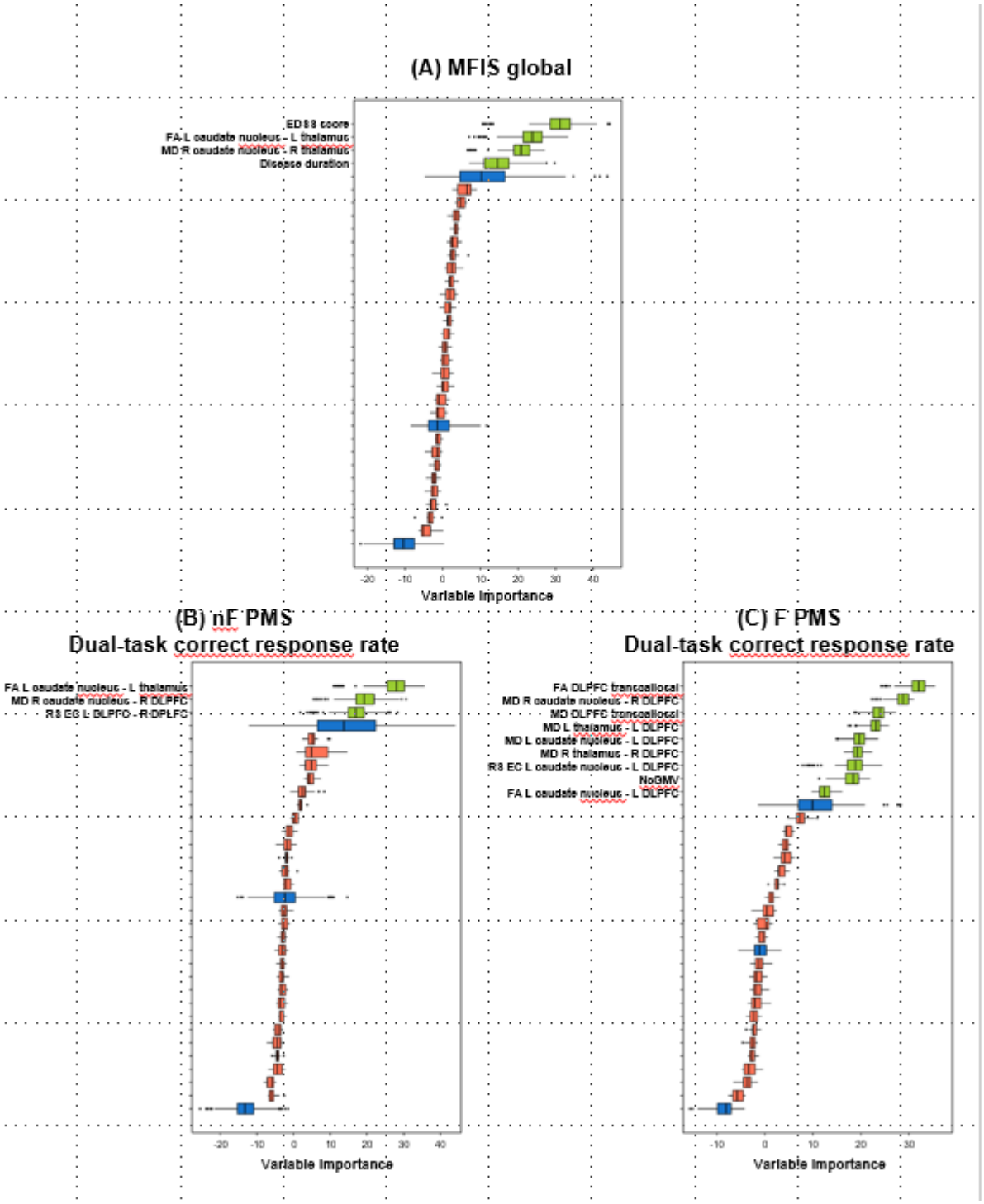
(A) MFIS global
EDSS score
FA L caudate nucleus - L thalamus
MD R caudate nucleus - R thalamus
Disease duration
-20 -10 0 10 20 30 40
Variable Importance
(B) nF PMS
Dual-task correct response rate
FA L caudate nucleus - L thalamus
MD R caudate nucleus - R DLPFC
RS EC L DLPFC - R DPLFC
-20 -10 0 10 20 30 40
Variable Importance
(C) F PMS
Dual-task correct response rate
FA DLPFC transcallosal
MD R caudate nucleus - R DLPFC
MD DLPFC transcallosal
MD L thalamus - L DLPFC
MD L caudate nucleus - L DLPFC
MD R thalamus - R DLPFC
RS EC L caudate nucleus - L DLPFC
NoGMV
FA L caudate nucleus - L DLPFC
-10 0 10 20 30
Variable Importance

Supplementary Material

Supplementary Methods

MRI acquisition. Using 3.0 Tesla scanners (IRCCS San Raffaele: Philips Ingenia CX; University of Genoa and University of Alabama: Siemens Prisma; Kessler Foundation: Siemens Skyra) and standardized procedures for subjects positioning, the following brain MRI sequences were acquired from all subjects during a single session: a) axial T2*-weighted single-shot EPI for resting state (RS) functional (f) MRI (all scanners: TR=1560 ms; TE=35 ms, flip angle=70°; multi-band factor=2, matrix size=96×96; FOV=240 x 240 mm^2; 48 contiguous axial slices, 3 mm thick, number of volumes=320); b) variable flip angle 3D T2-weighted fluid-attenuated inversion recovery (FLAIR) turbo spin echo (Philips scanner: repetition time [TR]=4800 ms; echo time [TE]=270 ms; inversion time [TI]=1650 ms; matrix size=256 × 256; field of view [FOV]=256 × 256 mm^2; echo train length [ETL]=167; 192 contiguous sagittal slices, 1 mm thick; Siemens scanners: TR=5000 ms; TE=395 ms; TI=1800 ms; matrix size=256 × 256; FOV=256 × 256 mm^2; ETL=284; 192 contiguous sagittal slices, 1.05 mm thick), c) sagittal 3D T1-weighted sequence: (Philips scanner: TR=7 ms; TE=3.2 ms; TI=1000 ms; flip angle=8°; matrix size=256 × 256; FOV=256 × 256 mm^2; 204 contiguous sagittal slices, 1 mm thick; Siemens scanners: TR=2300 ms; TE=2.98 ms; TI=900 ms; flip angle=9°; matrix size=256 × 256; FOV=256 × 256 mm^2; 204 contiguous sagittal slices, 1 mm thick); and d) axial pulsed-gradient spin echo single shot diffusion-weighted echo planar imaging (EPI) (all scanners: 3 shells at b-value=700/1000/2855 s/mm^2 along 6/30/60 non-collinear directions and 10 b=0 volumes were acquired, FOV=240×233 mm, pixel size=2.14×2.69 mm, 56 slices, 2.3 mm-thick, matrix=112×85, TR=about 6000 ms, TE=about 80 ms and three additional b=0 volumes with reversed polarity of gradients for distortion correction). Acquisition for RS fMRI scans required about 8 minutes. During RS fMRI acquisition, subjects were asked to keep their eyes closed, to remain motionless and not to think of anything in particular. All subjects stated that they had not fallen asleep during scanning, according to a

questionnaire delivered immediately after the MRI session. The total duration of MRI acquisition was approximately 50 minutes.

Voxel-wise atrophy analysis. Voxel-based morphometry (VBM), as implemented in SPM12 (www.fil.ion.ucl.ac.uk/spm), was used to map modifications in regional gray matter (GM) volumes between multiple sclerosis (MS) patients and healthy controls (HC). The lesion-filled 3D T1-weighted images were used for a group-wise alignment: first, the images were segmented into different tissue types via the Segmentation routine in SPM12. Then, GM and white matter (WM) segmented images of all study participants, in the closest possible rigid-body alignment with each other, were used to produce GM and WM templates and to drive the deformation to the templates. At each iteration, the deformations, calculated using the Diffeomorphic Anatomical Registration using Exponentiated Lie algebra (DARTEL) registration method [1], were applied to GM and WM, with an increasingly good alignment of study participant's morphology, to produce templates. Finally, an affine transformation that maps from the population average (DARTEL Template space) to Montreal Neurological Institute (MNI) space was calculated. GM and WM maps were spatially normalized, modulated for the Jacobian of the non-linear transformation and smoothed with an 8 mm Gaussian kernel. To define the DLPFC, Brodmann areas (BA) 9 and 46 were selected by BAs template (in which the DLPFCs are contained). For each study participant, the regional GM volume in the native space was obtained by summing values of the aforementioned maps within the mask.

DT MRI pre-processing. Preprocessing of diffusion-weighted imaging data included correction for off-resonance and eddy current induced distortions, as well as for slice-to-volume and subject movements, and signal dropout, using the Eddy tool within the FSL library (FSL version 6.0.1, www.fmrib.ox.ac.uk) [2].

The diffusion tensor (DT) was estimated in each voxel using the shell at b=700 and 1000 by linear regression [3] using the FMRIB's Diffusion Toolbox (FDT tool, FSL 5.0.5).

Construction of WM Atlas. To generate WM fiber bundles, a separate cohort of 44 HC (24 females, age 32 ± 12, range 18-55 years) underwent the same diffusion-weighted and 3D T1-

weighted MRI protocol described above, on the same 3.0 Tesla Philips Ingenia CX scanner used for the study at IRCCS San Raffaele.

Fiber orientation distribution (FOD) functions were computed using Multi-Shell, 3-Tissue Constrained Spherical Deconvolution, with group averaged response functions for WM, GM, and CSF using MRtrix3 software (www.mrtrix.org) [4]. FOD images of HC were averaged to create a study specific unbiased FOD population template. Spatial correspondence with the population template was achieved with an iterative registration and averaging approach [5]. Each subject's FOD and FA images were then registered to the template via a FOD-guided non-linear registration [6]. Probabilistic tractography[7] was then run using the FOD template to reconstruct the following WM tracts, which have been implicated in fatigue,[8-10] using a region of interest (ROI) approach and seed from the GM-WM interface: transcallosal fibers between left and right DLPFC, connections between ipsilateral caudate nucleus and thalamus, connections between ipsilateral caudate nucleus and DLPFC and connections between ipsilateral thalamus and DLPFC. For each WM tract, this approach is based on manual delineation of a "seed" ROI, based on anatomical landmarks (combining information provided by FA, FOD and T1-weighted images). Starting from the seed ROI, tractography reconstructs a probability map of the WM tract. An "end" ROI, namely another anatomical landmark to which the tract is known to connect the seed ROI was also used. Further "exclusion" ROIs were used to avoid the selection of undesired fibers and to optimize the selection of the tract of interest.

In details, the following seed and end ROIs were used for each WM tract:

- Transcallosal fibers between left DLPFC-right DLPFC: the spherical ROIs (10mm diameter) of DLPFC were shaped onto the BAs 46 and 9; the center of the left one: X:-42; Y:32; Z:30; and the right one: X: 42; Y:32; Z:30, in line with what suggested in a previous publication;[11]

- WM tracts connecting ipsilateral caudate nucleus-thalamus (left and right sides): the ROIs of these nuclei were the masks derived from FSL FIRST tool;

- WM tracts connecting ipsilateral caudate nucleus-DLPFC (left and right sides): the ROIs of caudate nuclei were derived from FSL FIRST tool, whereas the spherical seed ROIs (10mm diameter) of DLPFCs were shaped onto the BAs 46 and 9, as described above;

- WM tracts connecting ipsilateral thalamus-DLPFC (left and right sides): the ROIs of thalami were derived from FSL FIRST tool, whereas the spherical seed ROIs (10mm diameter) of DLPFCs were shaped onto the BAs 46 and 9, as described above.

For the subsequent analyses, mean FA and MD values of the aforementioned WM tracts were extracted by applying each atlas section as a mask on DWI of every single study participant.

RS fMRI pre-processing. RS fMRI data were pre-processed using the CONN toolbox (https://web.conn-toolbox.org/).[12] RS fMRI images were realigned to the mean of each session with a six-degree rigid-body transformation to correct for minor head movements. After rigid registration of realigned images to the lesion filled 3D T1-weighted scan, RS fMRI images were normalized to the MNI template using a standard affine transformation followed by non-linear warping. After detection of outliers (using the ART toolbox), images were smoothed with a 6 mm3 Gaussian filter. The five principal components derived from WM and CSF estimated with the anatomical component-based noise correction method (aCompCor),[13] and motion parameters with their first temporal derivatives were regressed out from RS fMRI time series as nuisance covariates. Outliers detected by the ART toolbox (if any) and spurious effects from the first two timepoints (to maximize magnetic equilibrium) were also regressed out from data. Finally, images were linearly detrended and band-pass filtered (0.01-0.1 Hz).

Supplementary References

1. Ashburner J. A fast diffeomorphic image registration algorithm. Neuroimage. 2007;38(1):95-113.
2. Andersson JLR, Graham MS, Drobnjak I, Zhang H, Filippini N, Bastiani M. Towards a comprehensive framework for movement and distortion correction of diffusion MR images: Within volume movement. Neuroimage. 2017;152:450-66.
3. Basser PJ, Mattiello J, Lebihan D. Estimation of the Effective Self-Diffusion Tensor from the Nmr Spin-Echo. J Magn Reson Ser B. 1994;103(3):247-54.
4. Jeurissen B, Tournier JD, Dhollander T, Connelly A, Sijbers J. Multi-tissue constrained spherical deconvolution for improved analysis of multi-shell diffusion MRI data. Neuroimage. 2014;103:411-26.
5. Raffelt D, Tournier JD, Fripp J, Crozier S, Connelly A, Salvado O. Symmetric diffeomorphic registration of fibre orientation distributions. Neuroimage. 2011;56(3):1171-80.
6. Raffelt D, Tournier JD, Crozier S, Connelly A, Salvado O. Reorientation of fiber orientation distributions using apodized point spread functions. Magn Reson Med. 2012;67(3):844-55.
7. Tournier JD, Calamante F., Connelly A. Improved probabilistic streamlines tractography by 2 nd order integration over fibre orien-tation distributions. 2009.
8. Arm J, Ribbons K, Lechner-Scott J, Ramadan S. Evaluation of MS related central fatigue using MR neuroimaging methods: Scoping review. J Neurol Sci. 2019;400:52-71.
9. Bertoli M, Tecchio F. Fatigue in multiple sclerosis: Does the functional or structural damage prevail? Mult Scler. 2020;26(14):1809-15.
10. Filippi M, Preziosa P, Rocca MA. Brain mapping in multiple sclerosis: Lessons learned about the human brain. Neuroimage. 2019;190:32-45.
11. Jaeger S, Paul F, Scheel M, Brandt A, Heine J, Pach D, et al. Multiple sclerosis-related fatigue: Altered resting-state functional connectivity of the ventral striatum and dorsolateral prefrontal cortex. Mult Scler. 2019;25(4):554-64.
12. Whitfield-Gabrieli S, Nieto-Castanon A. Conn: a functional connectivity toolbox for correlated and anticorrelated brain networks. Brain Connect. 2012;2(3):125-41.
13. Behzadi Y, Restom K, Liau J, Liu TT. A component based noise correction method (CompCor) for BOLD and perfusion based fMRI. Neuroimage. 2007;37(1):90-101.